

**ANTIMONY TELLURIDE AS A SATURABLE
ABSORBER FOR GENERATING Q-SWITCHED AND
MODE-LOCKED ERBIUM-DOPED FIBER LASERS**

ZEYAD ABDULLATEEF IBRAHEEM AL-DABAGH

FACULTY OF ENGINEERING

UNIVERSITY OF MALAYA

KUALA LUMPUR

2018

**ANTIMONY TELLURIDE AS A SATURABLE
ABSORBER FOR GENERATING Q-SWITCHED AND
MODE-LOCKED ERBIUM-DOPED FIBER LASERS**

ZEYAD ABDULLATEEF IBRAHEEM AL-DABAGH

**RESEARCH REPORT SUBMITTED IN FULFILLMENT
OF THE REQUIREMENT FOR THE MASTER DEGREE
IN TELECOMMUNICATION ENGINEERING**

FACULTY OF ENGINEERING

UNIVERSITY OF MALAYA

KUALA LUMPUR

2018

UNIVERSITY OF MALAYA
ORIGINAL LITERARY WORK DECLARATION

Name of Candidate: Zeyad Abdullateef Ibraheem Al-Dabagh

(I.C/Passport No:

Registration/Matric No: KQH160001

Name of Degree: MASTER OF TELECOMMUNICATION ENGINEERING

Title of Project Paper/Research Report/Dissertation/Thesis ("this Work"): Antimony Telluride as a saturable absorber for generating Q-switched and mode-locked erbium-doped fiber lasers

Field of Study: Photonic engineering

I do solemnly and sincerely declare that:

- (1) I am the sole author/writer of this Work;
- (2) This Work is original;
- (3) Any use of any work in which copyright exists was done by way of fair dealing and for permitted purposes and any excerpt or extract from, or reference to or reproduction of any copyrighted work has been disclosed expressly and sufficiently and the title of the Work and its authorship have been acknowledged in this Work;
- (4) I do not have any actual knowledge nor do I ought reasonably to know that the making of this work constitutes an infringement of any copyright work;
- (5) I hereby assign all and every right in the copyright to this Work to the University of Malaya ("UM"), who henceforth shall be owner of the copyright in this Work and that any reproduction or use in any form or by any means whatsoever is prohibited without the written consent of UM having been first had and obtained;
- (6) I am fully aware that if in the course of making this Work I have infringed any copyright whether intentionally or otherwise, I may be subject to legal action or any other action as may be determined by UM.

Candidate's Signature

Date:

Subscribed and solemnly declared before,

Witness's Signature

Date:

Name:

Designation:

Antimony Telluride as a saturable absorber for generating Q-switched and mode-locked erbium-doped fiber lasers

ABSTRACT

In this research, passively Q-switched and mode-locked erbium-doped fiber lasers (EDFLs) were experimentally demonstrated by using Antimony Telluride (Sb_2Te_3) Topological Insulator (TI) as a thin film based saturable absorber (SA). Liquid phase exfoliation (LPE) method was used to fabricate the SA by embedding the Sb_2Te_3 into polyvinyl alcohol (PVA) film. The pulse train was achieved by using a simple laser cavity designed to generate a low threshold pump power that creates significant pulse energy and peak power. Two experiments were conducted in this study. At first, a Q-Switching pulse laser was produced at the 1530.749 nm wavelength region. The Q-switched stabilized pulse laser was established with a threshold pump power as low as 15 mW. Repetition rate of the laser increased from 27.53 to 95.06 kHz, while the pulse width decreased from 13.84 μs to 4.89 μs as the pump power was raised from 15 mW to 81 mW. The maximum pulse energy of 45.87 nJ was obtained at the maximum pump power. By adding an additional single mode fiber (SMF) section into the laser cavity, the mode-locked pulse train was generated that operates at 1533.40 nm wavelength with 3 dB bandwidth of 2.7 nm. The mode-locked pulse laser was stabilized at pump power range of 71 mW to 143 mW with pulse width and repetition rate of 6.52 ps and 996 kHz, respectively. At the maximum pump power of 143 mW, the average output power, pulse energy, peak power and the signal to noise (SNR) ratio were 6.5 mW, 6.526 nJ, 1 kW and 67 dB respectively.

Keywords: Q-switched, Mode-Locked, Antimony Telluride.

Antimony Telluride as a saturable absorber for generating Q-switched and mode-locked erbium-doped fiber lasers

ABSTRAK

Dalam penyelidikan ini, erbium terdop gentian laser (EDFLs) Q -Suis dan mod-selakan pasif ditunjukkan secara eksperimen dengan menggunakan Telurid Antimoni (Sb_2Te_3) Penebat Topologi (TI) sebagai filem nipis penyerap tertepu (SA). Kaedah pengelupasan fasa cecair (LPE) digunakan untuk hasilkan SA dengan membenamkan Sb_2Te_3 ke dalam filem alcohol polivinil (PVA). Deretan denyut telah dicapai dengan menggunakan rongga laser ringkas yang direka bagi mendapatkan kuasa pam ambang rendah yang menghasilkan tenaga denyut dan kuasa puncak yang penting. Dua eksperimen telah dijalankan dalam kajian ini. Pertama, laser denyut Q-Switching dihasilkan di kawasan panjang gelombang 1530.749nm. Denyut Q-Suis yang stabil dihasilkan dengan kuasa pam ambang serendah 15 mW. Ia telah diperolehi dengan kadar ulangan bagi laser meningkat dari 27.53 hingga 95.06 kHz, manakala lebar denyut menurun daripada 13.84 μs ke 4.89 μs ketika kuasa pam ditingkatkan daripada 5 mW ke 81mW. Tenaga denyut yang 45.87nJ telah diperolehi pada kuasa pam maksimum. Dengan menambahkan keratan gentian mod tunggal (SMF) tambahan ke dalam rongga laser, denyut-denyut mod-selakan dijana untuk beroperasi di kawasan panjang gelombang 1533.40 nm dengan lebar jalur 3dB bagi 2.7nm. Laser denyut yang mod-selakan dimantapkan dalam lingkungan kuasa pam 71 mW kepada 143 mW dengan lebar denyut dan kadar ulangan 6.52 ps dan 996 kHz masing-masing. Pada kuasa pam maksimum 143mW, kuasa keluaran purata, tenaga denyut, puncak, dan isyarat kepada nisbah hingar (SNR) ialah 6.5 mW, 6.526 nJ, 1kW, dan 67 dB masing-masing.

ACKNOWLEDGEMENTS

I express my deepest gratitude and profound respect to all those who gave me the possibility to complete my research project. Firstly, I would like to thank my supervisor, Prof. Ir. Dr. Sulaiman Wadi Harun, who inspired and guided me to complete this research all along the way.

Besides my advisor, my appreciation goes to the rest of my thesis committee, Dr. Mahmoud Ahmed and Dr. Ahmed Al-Masoodi who patiently answered all the questions, endowed their valuable time to provide me with feedback and advice, discussed any problems and supported me at every stage of this research.

Furthermore, my sincere gratefulness goes to Dr. Anas Bin Abdul Latiff at Photonic Research Center (PRC) for his constant encouragement and illuminating thoughts that assisted me in my experiment.

Last but not least, I would like to thank my parents, whose love and guidance are with me in whatever I pursue, as well as to all my friends for their support during my work on this research.

Thank you very much, everyone

TABLE OF CONTENTS

Abstract	iv
Abstrak	v
Acknowledgements	vi
Table of Contents	vii
List of Figures	ix
List of Symbols and Abbreviations	xi
CHAPTER 1: INTRODUCTION	1
1.1 Background	1
1.2 Problem Statement and Research Motivation	2
1.3 Objectives of this study	4
1.4 Report Outline	4
CHAPTER 2: LITERATURE REVIEW	5
2.1 Introduction	5
2.2 Laser Structure	6
2.3 Laser Operation	6
2.4 Erbium-Doped Fiber Laser (EDFLs)	8
2.5 Saturable Absorber (SA)	10
2.6 Topological Insulator	12
2.7 Overview of Q-switching Technique	15
2.8 Overview of Mode-Locking Technique	18
2.9 Liquid Phase Exfoliation (LPE) Technique	19
2.10 Optical Measurement	20
2.10.1 Repetition Rate and Pulse Duration	21

2.10.2 Pulse Energy.....	22
2.10.3 Peak Power.....	22
CHAPTER 3: GENERATING Q-SWITCHED ERBIUM-DOPED FIBER LASERS USING ANTIMONY TELLURIDE SA.....	23
3.1 Introduction.....	23
3.2 Characterization and Fabrication of Antimony Telluride Sb_2Te_3	23
3.3 Laser Cavity Setup.....	27
3.4 Q-switched pulse laser performance.....	29
3.5 Summary.....	33
CHAPTER 4: GENERATING MODE-LOCKING ERBIUM-DOPED FIBER LASERS USING ANTIMONY TELLURIDE SA	34
4.1 Introduction.....	34
4.2 Mode-Locked EDFL Setup and its performance.....	34
4.3 Summary.....	40
CHAPTER 5: CONCLUSION.....	41
References.....	43
List of Publications and Papers Presented	47

LIST OF FIGURES

Figure 2.1: CW and pulses emission.....	5
Figure 2.2: A basic setup of the laser resonator	6
Figure 2.3: Laser operations.....	7
Figure 2.4: Various energy level: (a) Ytterbium (Yb^{3+}), (b) Erbium (Er^{3+}) and (c) Neodymium (Nd^{3+})	8
Figure 2.5: The operation of three levels fiber laser	9
Figure 2.6: The operation of SA	10
Figure 2.7: The crystal structure of (a) Bi_2Se_3 and (b) Bi_2Te_3	13
Figure 2.8: Raman spectra of Bi_2Se_3 and Bi_2Te_3	13
Figure 2.9: Crystal structure of Sb_2Te_3	14
Figure 2.10: Active Q-switching technique manipulation	16
Figure 2.11: Passive Q-switching laser generation	16
Figure 2.12: Mode-lock Operations	18
Figure 2.13: The solvothermal exfoliation processes	20
Figure 2.14: Repetition rate and pulse duration	22
Figure 3.1: Fabrication processes of Antimony Telluride Sb_2Te_3	24
Figure 3.2: Optical characteristics of the Sb_2Te_3 –PVA (FESEM image).....	25
Figure 3.3: Linear absorption spectrum	25
Figure 3.4: Raman spectrum	26
Figure 3.5: Nonlinear transmission	27
Figure 3.6: The ring cavity schematic diagram of the Q-Switched pulse laser with 4.9m total length.....	28
Figure 3.7: The fiber connectors of experiment with Sb_2Te_3 SA	28
Figure 3.8 Stability of the Q-switching operations at 1533 nm wavelength.....	30

Figure 3.9: Oscilloscope train at pump power of 15 mW, 41 mW and 81 mW	30
Figure 3.10: Pulse width and repetition rate at a various levels of the pump power.	31
Figure 3.11: Pump power stability with 5.83% slope efficiency of pulse energy and output power.....	31
Figure 3.12: Peak power and pulse duration corresponding to the pump power.....	32
Figure 3.13: RF spectrum measurement	32
Figure 4.1: The ring cavity schematic diagram of the mode-locked pulsed laser with 201m total length.....	35
Figure 4.2: Mode-locked is operated at 1533.40 nm wavelength - 2.7 nm FWHM	37
Figure 4.3: Oscilloscope output at maximum pump power	37
Figure 4.4: Autocorrelator pulse duration of 6.52 ps.....	38
Figure 4.5: Pulse energy and output power with 4.51% slope efficiency during mode-locked operations	38
Figure 4.6: Repetition rate stability associated with pump power	39
Figure 4.7: RF spectrum measurement with 66.76 dB SNR.....	39

LIST OF SYMBOLS AND ABBREVIATIONS

ASE	:	Amplified Spontaneous Emission
ARPES	:	Angle-Resolved Photoemission Spectroscopy
Sb ₂ Te ₃	:	Antimony telluride
P _{avg}	:	Average power
Bi ₂ Se ₃ ,	:	Bismuth Selenide
Bi ₂ Te ₃ ,	:	Bismuth Telluride
CO ₂	:	Carbon Dioxide
CW	:	Continuous Wave
<i>E</i>	:	Energy
Er ³⁺	:	Erbium
EDFL	:	Erbium-Doped Fiber Laser
FESEM	:	Field Emission Scanning Electron Microscopy
<i>F</i>	:	Frequency
FWHM	:	Full Width at Half Maximum
GaAs	:	Gallium Arsenide
GVD	:	Group Velocity Dispersion
GO	:	Graphene Oxide
He-Ne	:	Helium-Neon
LD	:	Laser Diode
η	:	Laser efficiency or slop efficiency
LASER	:	Light Amplification by Stimulated Emission of Radiation
MBE	:	Molecular Beam Epitaxy
Nd ³⁺	:	Neodymium
Nd:YAG	:	Neodymium-Doped Yttrium Aluminium Garnet

OSA	:	Optical Spectrum Analyzer
OSC	:	Oscilloscope
P _{out}	:	Output Power
P _p	:	Peak power
PC	:	Polarization Controller
PVA	:	Polyvinyl Alcohol
P	:	Power
PE	:	Pulse energy
T	:	Pulse period
PRR	:	Pulse Repetition Frequency
Δt	:	Pulse-durations (Pulse-width)
R _r	:	Repetition rate
SA	:	Saturable Absorber
SESAMs	:	Semiconductor Saturable Absorber Mirrors
SNR	:	Signal to Noise Ratio
SMF	:	Single Mode Fiber
SWCNTs	:	Single-Walled Carbon Nanotube
C	:	Speed of light
TI	:	Topological Insulator
TMDs	:	Transition Metal-Doped Crystals
Yb ³⁺	:	Ytterbium
WDM	:	Wavelength Division Multiplexer

CHAPTER 1: INTRODUCTION

1.1 Background

During the last two decades, the innovation and the rapid development of photonic have become crucial in enhancing laser performance. The laser characteristics include the coherent, monochromatic, high intensity and directional (Aruldas & Rajagopal, 2005), can be calibrated for specific needs. All these properties provide a significant beam of optical radiation within ultra-fast and ultra-short pulse lasers. Moreover, the novelty of both absorption properties and nonlinear optical effects are important factors in improving the pulse laser operation. Fiber laser is considered vital in the field of engineering technology, which has wide appliance especially in science and practical applications. Over recent years, the development of Erbium-doped fiber lasers (EDFLs) has assisted in the implementation and employment of the sensor applications and optical communication (DeCusatis & DeCusatis, 2010). Different laser applications have progressed by using the active technique or passive technique. The active technique can be generated by applying an optical modulation device into the optical cavity setup. Nevertheless, cost and complexity are some barriers to the use of this modulation. On the other hand, the passive technique relies on the saturable absorber (SA), which provides a simple and cheap approach to produce a train of pulse laser. SA is a nonlinear optical material that can absorb the incidence light of low intensity. The pulse train is generated by Amplified Spontaneous Emission (ASE) when SA is placed inside the laser cavity. After several round trips, the high-intensity light passes through the SA and initiates light in the form of fast sequence pulses (Ter-Mikirtychev, 2014). In this report, mode-locked and Q-switched EDFLs are expounded using an Antimony Telluride (Sb_2Te_3) Topological Insulator (TI) as an SA.

1.2 Problem Statement and Research Motivation

Mode-locked and Q-switched fiber lasers are considered outstanding resources for numerous current photonic applications which provide a pulse train that can operate in a range of microseconds to femtoseconds. Medical, industry, advanced science and modern optical communication are applications that heavily use pulse lasers. This operation can be produced by utilizing SA to induce the loss modulation inside the cavity to generate both ultra-fast and ultra-short (passive Q-switched and mode-locked) fiber lasers. EDFLs uses the Erbium-doped fiber (EDF) as a gain medium that operates in the wavelength region from 1520 to 1620 nm. The EDF can be pumped by either 980nm or 1480 nm laser diode which produces a gain in the wavelength regions such as the C-Band or L-Band regions.

Over the past years, several SAs such as SESAMs (Keller, 2003), SWNTs (Martinez, Fuse, & Yamashita, 2013) and graphene (Popa et al., 2010), were intensively investigated for generating pulse lasers in both the C and L-band regions. Nevertheless, Semiconductor Saturable Absorber Mirrors have some limitations (such as cost and fabrication complexity. It is also limited by its narrow operation wavelength band).

SWCNTs SAs have also been widely used as they are cheaper and easier to fabricate. Nonetheless, the wavelength operation depends on the diameters of the nanotube. Ultra-fast recovery time and broadband saturable absorption are benefits of the Graphene (Kim, Cho, Jang, & Song, 2011; Luo et al., 2010; Popa et al., 2011). However, graphene has a low absorption co-efficiency (2.3%/layer) and an absence of band-gap, which is considered a weakness for most of fiber laser applications (Y. Chen et al., 2015).

Recently, the Antimony Telluride (Sb_2Te_3) SA has been investigated by many researchers for both mode-locking and Q-switching. This is due to its advantages such as fast recovery time, low saturation intensity and wide bandwidth operation. The Sb_2Te_3 SA has been reported to generate mode-locked pulses from EDFL cavity by implementing mechanical exfoliation (ME) technique (Bogusławski et al., 2016; J Sotor, Sobon, Grodecki, & Abramski, 2014; Jaroslaw Sotor, Sobon, Macherzynski, Paletko, & Abramski, 2015; Jaroslaw Sotor et al., 2014a). However, the ME method carries a number of limitations including its inability to obtain the yield requirements, its lack of scalability and the need for a skilled manual labor (Lin, Chui, Li, & Lau, 2017).

The Sb_2Te_3 SA is considered a new promising material which is valid for different applications. Until now, the novelty of this research is to utilize the Sb_2Te_3 SA as a thin film which can produce an ultra-short pulse laser. The thin film is fabricated by using the Liquid-phase exfoliation (LPE) method which provides an extreme simplicity and scalability for the SA performance (Gupta, Arunachalam, & Vasudevan, 2016). Furthermore, LPE (highlighted in chapter 2) provides 2D nanosheets with high crystallinity.

In this work, Q-switched and mode-locked EDFLs are demonstrated and proposed using the Antimony Telluride as the SA. The saturable absorber is applied into the laser cavity where the thin film of Antimony Telluride (Sb_2Te_3) is sandwiched between two fiber ferrules. The cavity was achieved a stable pulse train with a good repetition rate, pulse width and peak power. The performance of both techniques is discussed in this report.

1.3 Objectives of this study

This research aims to develop Q-switched and Mode-locked EDFLs by using Sb_2Te_3 Topological Insulator (TI) as a saturable absorber. This research is guided by the following objectives:

1. To fabricate and characterize Antimony Telluride (Sb_2Te_3) SA by LPE.
2. To experimentally perform and evaluate the Q-switched erbium-doped fiber lasers using Antimony Telluride (Sb_2Te_3) SA.
3. To generate and evaluate mode-locked erbium-doped fiber lasers using Antimony Telluride (Sb_2Te_3) SA.

1.4 Report Outline

This report describes the fundamental, working principle, experimental techniques and outcomes that the research have accomplished from the Q-switched and Mode-locked fiber laser using a Sb_2Te_3 SA. The Antimony Telluride is embedded into polyvinyl alcohol (PVA) to make a film. The SA film is inserted between two fiber connectors inside the ring cavity. The released pulse laser was in the range of 1550 nm by stimulating the SA.

This research report is structured into five chapters. Chapter one presents the introduction of pulsed fiber lasers, motivation and the objectives of this study. Chapter two provides a short literature review on saturable absorption, Q-switching and mode locking techniques. Chapter 3 focuses on the fabrication and characterization of the Sb_2Te_3 film. Besides, a discussion is given to the generation of the Q-switched fiber laser. Chapter four describes the generation of mode-locking pulse trains in EDFL cavity using the Sb_2Te_3 SA. Finally, chapter five provides a conclusion to summarize the important outcomes of this research.

CHAPTER 2: LITERATURE REVIEW

2.1 Introduction

Laser was first invented in the early 1960's and had become indispensable for most of the current photonic applications. With time, many inventors have further developed the laser in order to be applicable for most high-end applications with a different major, especially optical communication and sensor technology. In general, the propagation of fiber lasers is in the form either continuous wave (CW) or pulse mode (Gambling, 1992). In CW laser, the intensity of the light is constant, nonetheless, the pulse laser is a sequence of the pulse, as shown in figure 2.1. The pulse laser classified into either mode-locked or Q-switched pulses.

CW relies on two constant parameters including intensity and phase, whereas pulse lasers rely on peak power, pulse energy, repetition rate and pulse width. Since pulse lasers was introduced, it has taken over the CW laser and has been applied to several spheres as remote sensing including in the fields of medicine, optical communications and others (Ter-Mikirtychev, 2014). Moreover, most of the current long-distance data transmission is based on pulse laser characteristics especially in rural areas due to the minimum energy loss, short pulses duration and optical signal sustainability.

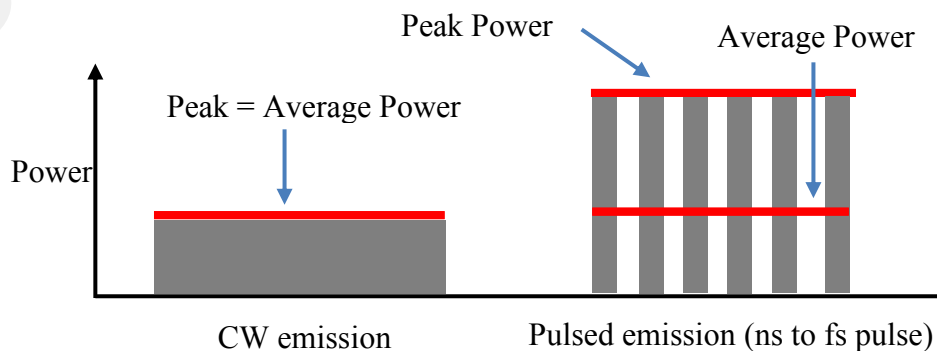


Figure 2.1: CW and pulses emission

2.2 Laser Structure

The basic structure of laser resonator consists of three components which are the gain medium, the mirrors and the power source, as shown in figure 2.2. The main component is the gain medium (laser medium) which contains atoms with electrons that may be excited to a metastable energy level by the processes of the stimulated emission (Siegman, 2000; Träger, 2012). Over the past couple of decades, various types of the gain medium have been invented. Examples include, Solid crystals such as ruby (Maiman, 1960), Nd:YAG, liquid dyes, gases like CO₂ (Patel, 1964) or Helium/Neon, or semiconductors such as GaAs (Chow & Koch, 2013). The high reflection mirror and the partially transmissive mirror are placed at both ends of the gain medium. The two mirrors allow the amplification of light goes back and forth. The last component refers to the pump source (electrical discharges, flash-lamps, or chemical reactions) that excites the atom to a metastable level in order to generate a state of population inversion.

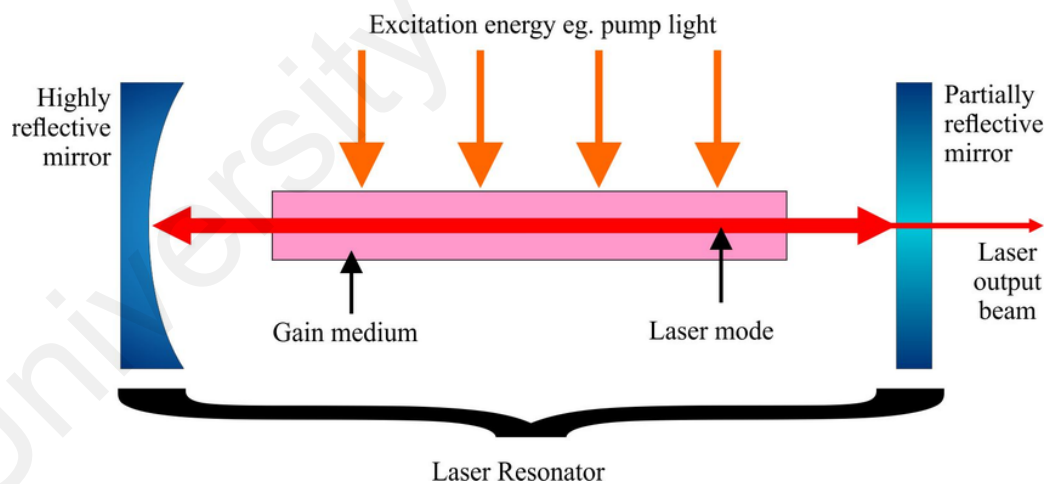


Figure 2.2: A basic setup of the laser resonator

2.3 Laser Operation

As a basic fundamental of the energy level of each atom which is based on the quantum theory, there is a specific level of energy for the individual atom. Generally, in a non-motivation situation, the atom remains on the E₁ level and is called ground-state level. In the state of an external excitation source or pumping, the relaxing atom electron (on the

lower level) excites by the input source which motivates the atom and excites it from the lower level E1 to the higher energy level E2, this process is known as absorption. After the very short duration, usually less than 1 second, the excited atoms fall down to E1 level. The atom in this case loses its energy and emits a photon but in a random direction. This step is called spontaneous emission.

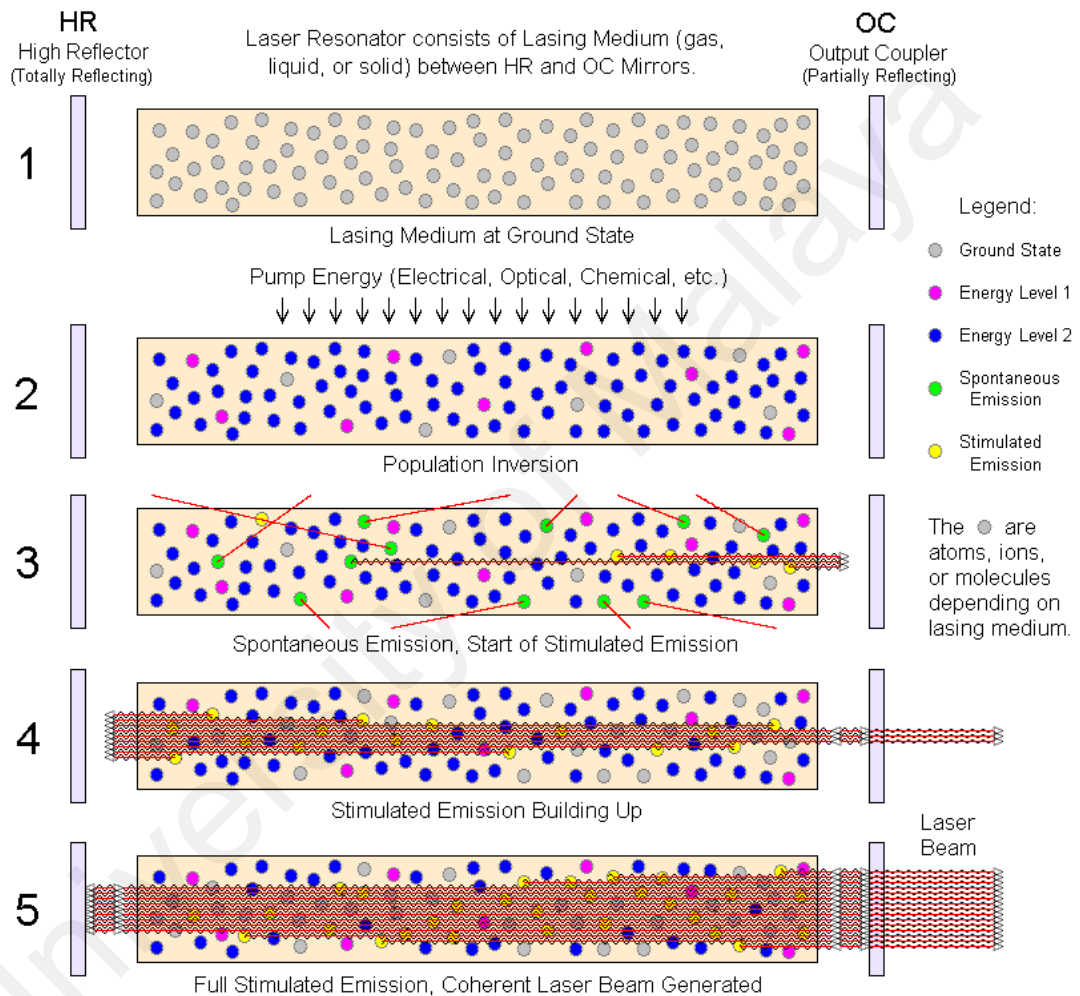


Figure 2.3: Laser operations

Furthermore, the atom at the E2 level collides with an external photon, the electron will lose its energy and will emit a photon that has the same wavelength and direction as the incidence photon. This process is called stimulated emission when $E2 - E1 = h * \nu$. Figure 2.3 shows the operation of two level of the energy system (Dong & Samson, 2016).

2.4 Erbium-Doped Fiber Laser (EDFLs)

A fiber laser uses rare-earth elements such as erbium as the gain medium, which is the place where the atom can be excited by the process of stimulated emission (Agrawal, 2010). In order to achieve the state of population inversion, which refers to the majority of more atoms or molecules are in a higher excited state. The population inversion operations require three or four levels of energy. Figure 2.4 shows the energy level diagram for three types of the laser (Yb^{3+} , Er^{3+} and Nd^{3+}) (L. Tian et al., 2014), the blue color refers to the pump and the red to the laser emission.

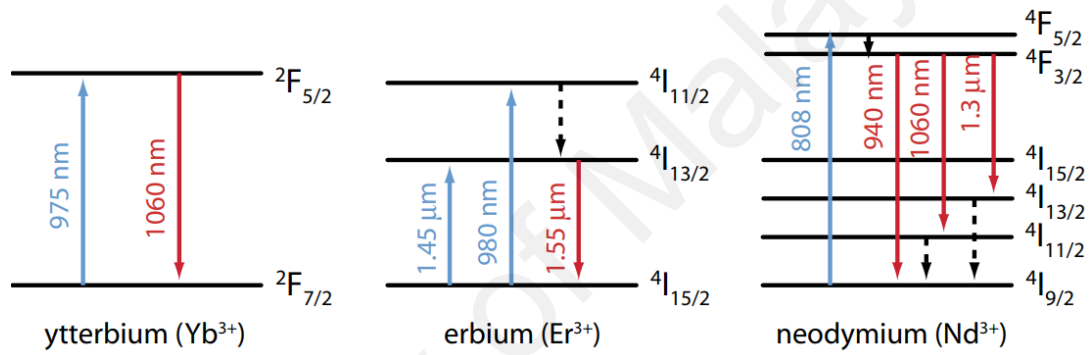


Figure 2.4: Various energy level: (a) Ytterbium (Yb^{3+}), (b) Erbium (Er^{3+}) and (c) Neodymium (Nd^{3+})

The 1.55 μm fiber laser can be produced by using the Erbium-doped fiber as the gain medium in conjunction with 980 nm and 1450 nm pumping (Agrawal, 2010). In the three-levels mode, each level is identified by a label. E1 represents the ground level, E2 level is the middle (metastable) level that has more transition lifetime compared to the E3 higher energy states. In general, 980 nm is a pump laser which is usually used in the three levels laser which generates the population inversion (Y.-C. Chen et al., 2002). Under normal conditions, ions remain at the ground level E1, the pump 980 nm excites the ions to a higher level. The duration of ions that are sustained at the E3 energy states is around 1 second, after that they decay to the intermediate level E2. At this stage, the excited

photon releases its energy as thermodynamic noise considerations (non-radiative emission). Spontaneous emissions occur when some of the ions decay from the intermediate metastable energy state to the ground energy band which can add noise to the system, as shown in figure. 2.5. Some of the photon in band-gap, between E1 and E2, motivate or excite the atom at the metastable state (Ter-Mikirtychev, 2014).

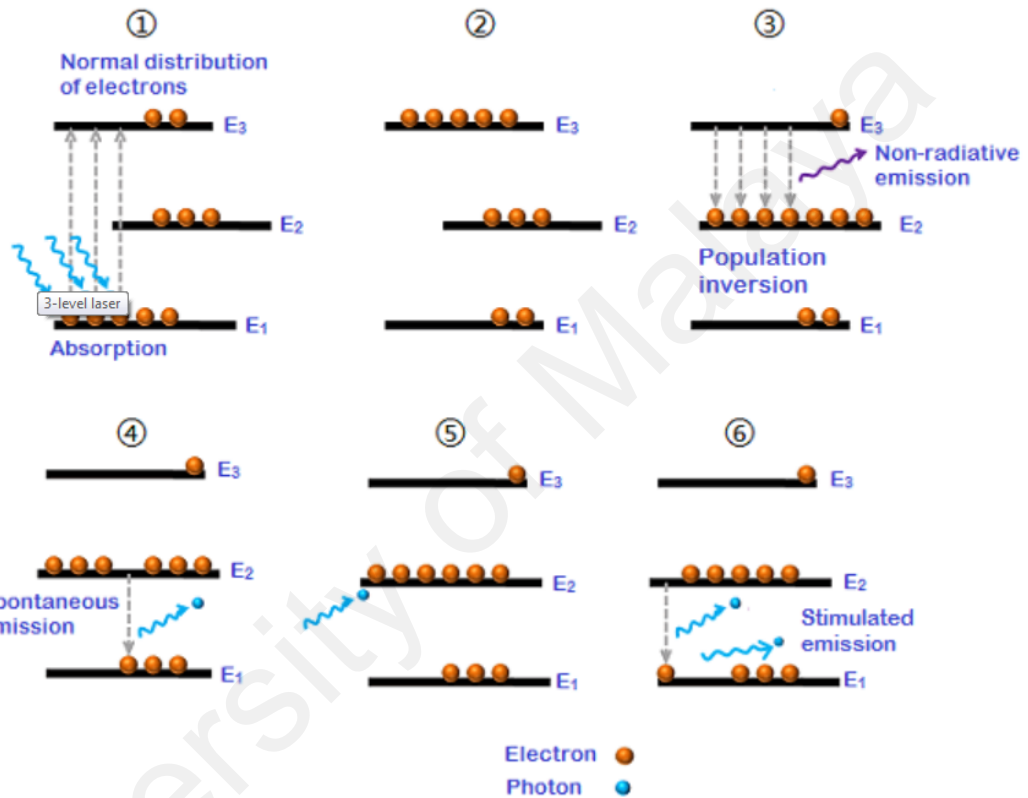


Figure 2.5: The operation of three levels fiber laser

Thus, two actions take place. Firstly, stimulated absorption occurs when some photons are absorbed by ions in the ground state, therefore, ions excite to E₂. Secondly, stimulated emission happens when a new incidence photons that have the same wavelength, energy and polarization encounter atoms in an upper energy level. The state of population inversion can occur when a significant number of atoms remain at the metastable state.

When the widths between the middle-level E2 and the ground band level increases, stimulated emission occurs between 1530 to 1560 nm (Y.-C. Chen et al., 2002).

2.5 Saturable Absorber (SA)

A saturable absorber is a nonlinear optical component that has some optical losses, which can affect the optical intensity of light. This can happen when a significant optical intensity leads to depletion of the ground state of these ions (Dutta, 2015). Figure 2.6 presents the operation of SA.

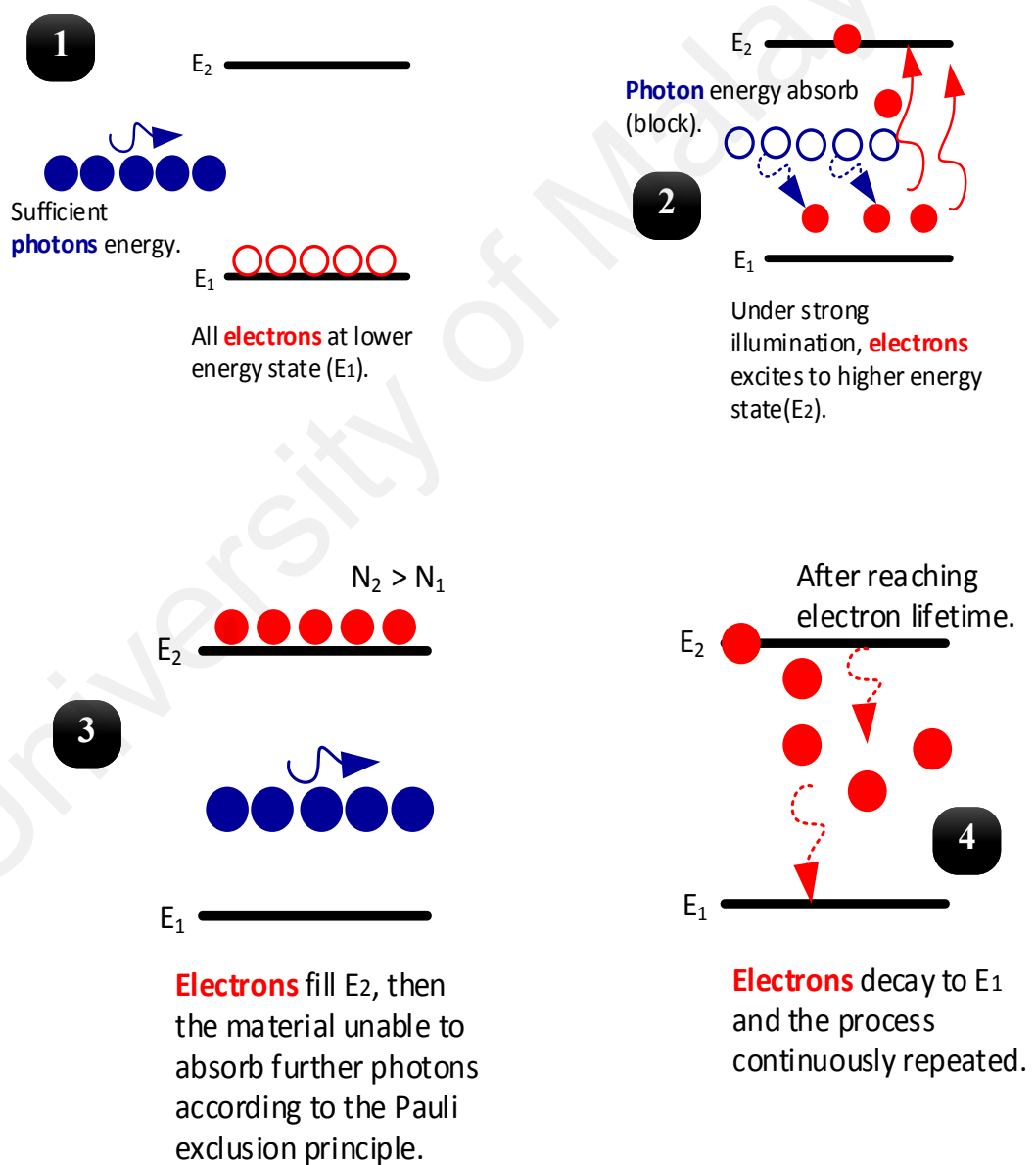


Figure 2.6: The operation of SA

Under the normal situation when there is no charge (external energy source), the electrons are at the low stage of energy (ground state) E1 as shown in step 1 above. When a sufficient incident light or energy occurs (under strong illumination), the majority of electrons are excited to a higher state level E2, as shown at stage 2. The population inversion occurs when the majority of electrons excite the E2. After short duration around ≈ 1 ns, when the SA is unable to absorb more photon, the electrons reach their lifetime and decay to ground level E1. This process is continually repeated and produces a photon that has the same phase as the incidence photon. This operation of the SA can help absorb the incidence light in order to generate ultra-short or ultra-fast pulses (DeCusatis & DeCusatis, 2010).

Beyond the novelty of saturable absorber, an outstanding optical pulse can generate, Q-switching and mode locking pulses are the main advantages of a saturable absorber. For the past years, implementing the SA resulted in the generation of many striking pulses. By using the rhodamine-based organic dye SA, a mode-locked pulse of 10 ns was obtained. Recently, several SAs such as the SESAMs (Keller, 2003), single wall carbon nanotubes (SWNTs) (Martinez et al., 2013), graphene (Popa et al., 2010) and graphene oxide (Jung et al., 2013) have been intensively investigated. The SESAMs and Transition metal-doped crystals (TMDs) (Pan, Utkin, & Fedosejevs, 2007) have achieved a great development and have been applied to various fields like industry and other commercial fields. Nevertheless, there are a number of limitations of SESAMs owing to its complexity, range operation and manufacturing difficulties of the molecular beam epitaxy (MBE) system.

Graphene is the first type of the two-dimensional (2D) material which was commonly proposed and demonstrated to produce both mode-locked and Q-switched pulse laser (Cizmeciyan et al., 2013; Jung et al., 2013; Pan et al., 2007; Popa et al., 2010). Graphene

has been confirmed to generate laser pulse due to the fact that it has a number of advantages such as its lower cost, low saturation intensity, ultra-fast recovery time and its ease to fabricate. Nonetheless, Graphene carries some limitations which degrade its performance such as its very low band-gap and its low absorption efficiency (Ahmed, 2016; Cizmeciyan et al., 2013).

2.6 Topological Insulator

Topological insulators are electronic materials that have a bulk band gap like an ordinary insulator but have protected conducting states on their edge or surface. These states are possible due to the combination of spin-orbit interactions and time-reversal symmetry. The three main stoichiometric crystals of TI materials are Bismuth (III) Selenide (Bi_2Se_3), Bismuth (III) Telluride (Bi_2Te_3) and Antimony Telluride (Sb_2Te_3). The Bi_2Se_3 and Bi_2Te_3 are binary chalcogenides of bismuth Bi_2X_3 with complex layer structures, as shown in Figure 2.7. The crystal structure of Bi_2Se_3 and Bi_2Te_3 can directly react with the elements at 500-900°C. Bi_2Se_3 and Bi_2Te_3 have small band gaps of 1.35 and 1.21 eV, respectively, so they exhibit semiconductor properties. They can be used in television cameras, optoelectronic and switching devices and thermoelectric refrigerator due to their properties as thermoelectric and semiconducting materials. These materials can be synthesized by physical or chemical methods (Kong et al., 2010). Chemical methods are widely used to prepare a thin film of TI materials due to the ease of fabrication and the large surface deposition (Anwar, Anwar, & Mishra, 2014).

For structure mode of TI materials, the vibration modes were detected in Raman spectra as reported by Liu et al. (Liu et al., 2011), which are three peaks for Bi_2Se_3 and two peaks for Bi_2Te_3 at a small range from 50- 200 cm^{-1} , as shown in Figure 2.8 (a and b).

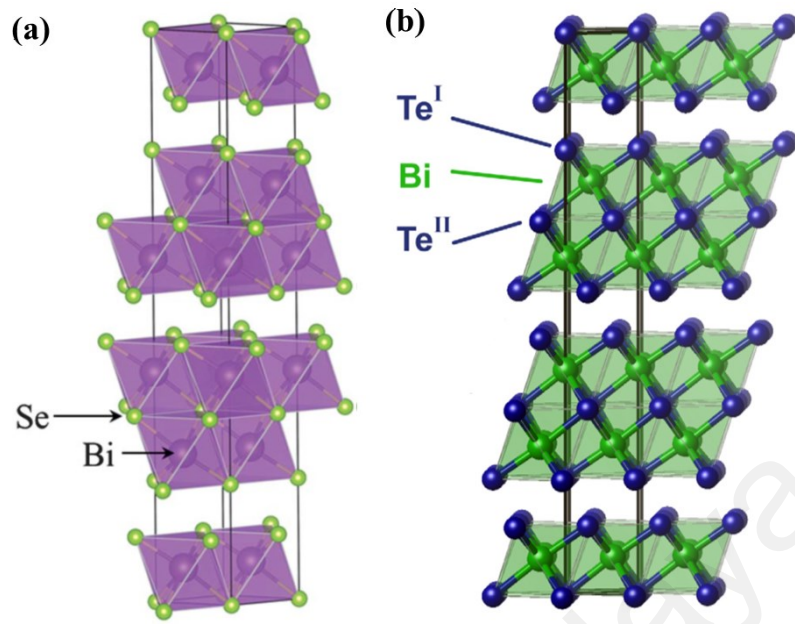


Figure 2.7: The crystal structure of (a) Bi₂Se₃ and (b) Bi₂Te₃

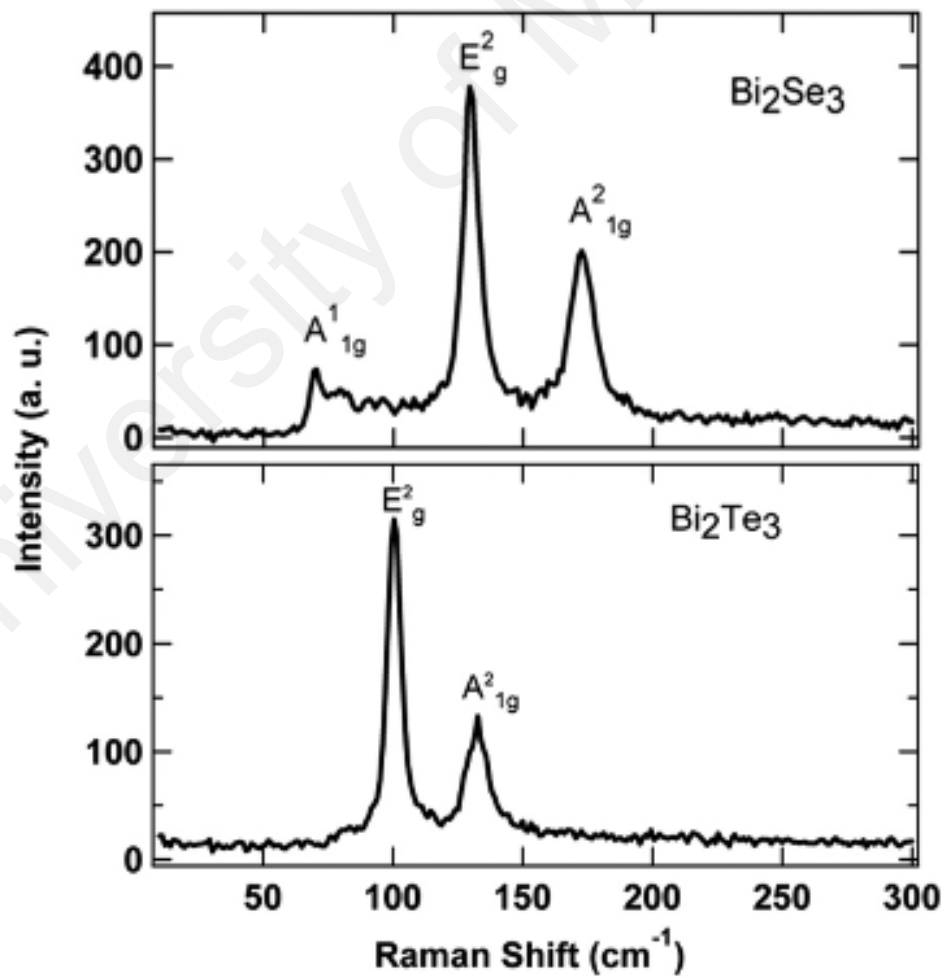


Figure 2.8: Raman spectra of Bi₂Se₃ and Bi₂Te₃

A recent investigation (Hasan & Moore, 2011) has illustrated the topological insulators (TI) in two dimensions which is under the nonmagnetic insulators. TI was determined by the angle-resolved photoemission spectroscopy (ARPES) method which has three types of SA's (Bi_2Te_3 , Bi_2Se_3 and Sb_2Te_3). This method observes the distribution of the electrons in the reciprocal space of solids. In TI, electrons can only move along the surface of the material. The uniqueness of TI lies in its surface states which is covered by conservation and time reversal symmetry that provide protection.

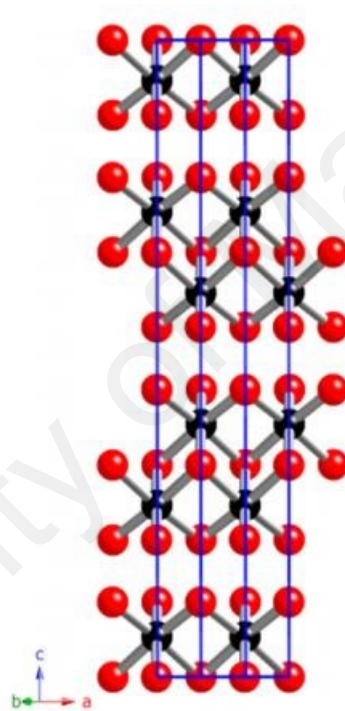


Figure 2.9: Crystal structure of Sb_2Te_3

The Sb_2Te_3 is considered a new promising material which is valid for a number of applications. Figure 2.9 illustrates the crystal structure of Antimony Telluride Sb_2Te_3 , which consists of two atomic sheets of antimony and three atomic sheets of tellurium.

In the last few years, the usage of Antimony Telluride (Sb_2Te_3) has attracted the attention of many researchers for mode-locking and Q-switching which generate pulse fiber lasers due to its full compatibility with optical characterization, its fast recovery time, low saturation intensity and wide bandwidth operation. The Sb_2Te_3 SA has

confirmed to generate mode-locked from erbium-doped fiber laser by implementing mechanical exfoliation technique (Popa et al., 2010; J Sotor et al., 2014; Jaroslaw Sotor et al., 2014b). However, the mechanical exfoliation technique suffers from low yield and low production rate, which is not scalable for practical applications (Lin et al., 2017). A mode-locked Yb-doped fiber has generated by using Antimony Telluride deposited D-shaped fiber (Kowalczyk et al., 2016). Nevertheless, the D-shaped has some limitations such as asymmetrical geometries that show a reasonable directional bend sensitivity. On another hand, solution-processed electronic devices are usually preferred due to their low cost, large area, flexibility and convenient materials integration.

The Sb_2Te_3 SA is considered a new promising material which is valid for different applications. Until now, the novelty of this research is to utilize the Sb_2Te_3 SA as a thin film which can produce an ultra-short pulse laser. The thin film is fabricated by using Liquid-phase exfoliation (LPE) method which provides an extreme simplicity and scalability for the SA performance (Gupta et al., 2016). Furthermore, LPE (highlighted in chapter 2) provides 2D nanosheets with high crystallinity.

2.7 Overview of Q-switching Technique

The Q-switching is a technique produces an energetic pulse laser usually within the range of nanoseconds to microseconds. This technique can be achieved by modulating the losses of the cavity. Basically, Q-switching can be classified into two main techniques: active or passive. The active Q-switching can be obtained by various mechanisms (Chang, Lee, & Lee, 2012). I.e. a mechanical device such as a shutter, chopper wheel, or spinning mirror/prism placed inside the cavity. It can also occur via an electro-optic device such as a Pockels cell (Strickland & Mourou, 1985) or a Kerr cell (McClung & Hellwarth, 1962) or a modulator such as an acousto-optic device (Savage, 2010). The changes of Q-

factor is associated with changes of resonator loss. The losses are modulated with an active control element. The Active technique can be achieved by adjusting the variable attenuator of the laser cavity (Mao & Lit, 2003).

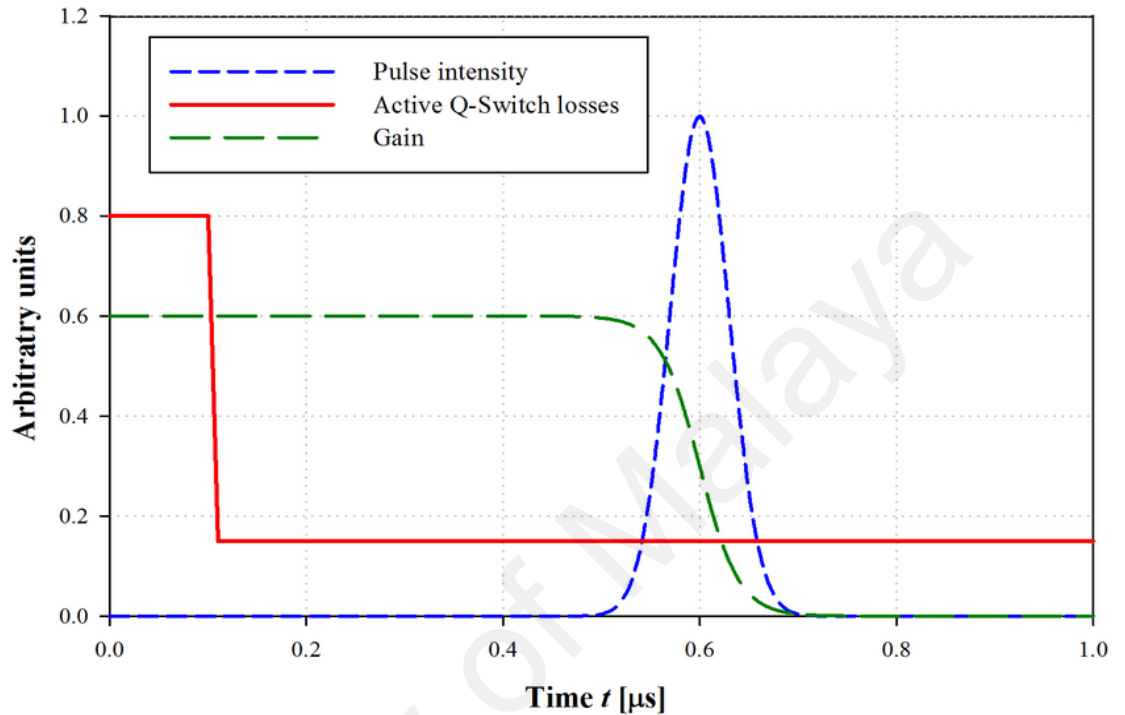


Figure 2.10: Active Q-switching technique manipulation

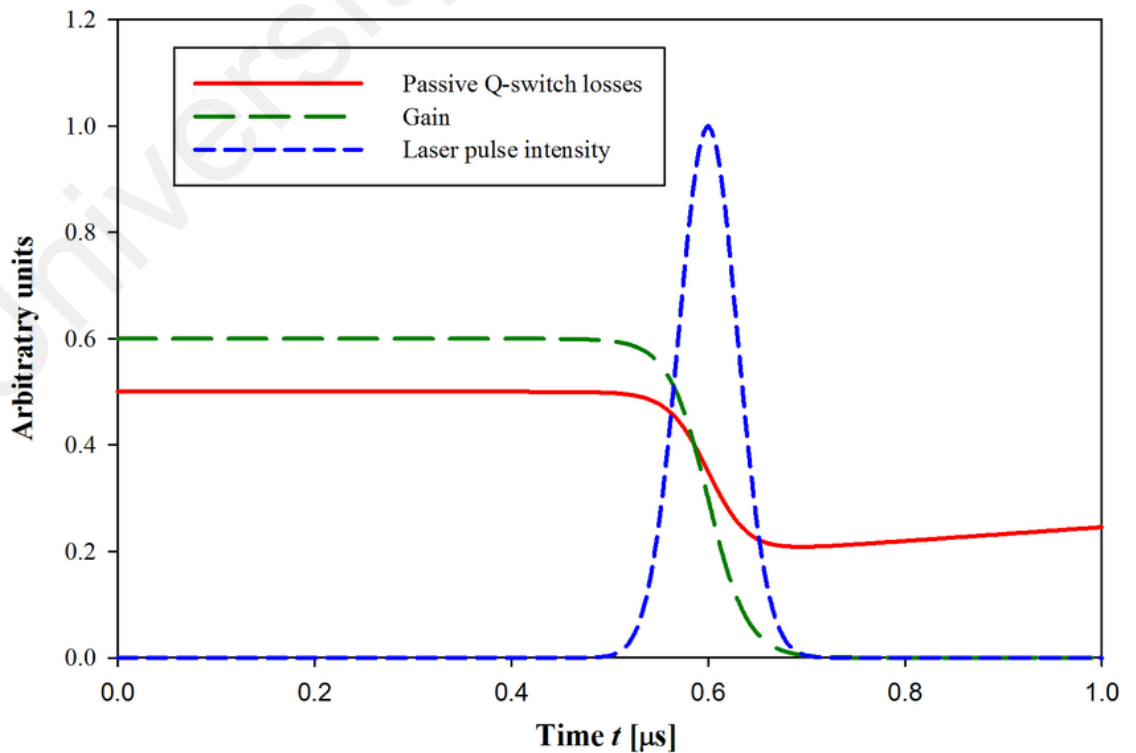


Figure 2.11: Passive Q-switching laser generation

Modulators contribute to a faster changing Q-factor that leads to a higher Q-factor. Thus, repetition rate can be easily controlled, as shown in figure 2.10. Nevertheless, the active technique has some disadvantages due to its complexity and cost as well as the alignment difficulties of modulators.

On the other hand, passive Q-switched fiber lasers are based on the saturable absorber which spontaneously modulates the losses of the laser cavity (Carruthers, Duling, & Dennis, 1994). SA provides a compact and simple way to generate a train of the short pulse laser. Placing SA within a resonator, inhibits laser oscillation due to the absorption loss it introduces. Figure 2.11 illustrates the contribution of the SA inside the laser cavity which minimizes the resonator losses corresponding to gain, thus, a significant pulse can be produced. Unlike active technique, the passive Q-switching is more cost-effective and less complex as it eliminates the use of modulators devices (X. Chen et al., 2014). Furthermore, the passive technique can produce a short pulse laser. Nonetheless, the high intensity of pulse energy can make the action more efficient than passive technique.

The first Q-switching was generated in 1958 by Gordon Gould (Bertolotti, 2015) followed by a solid-state laser (ruby) (Maiman, 1960). Hellwarth, (Hellwarth, 1961) suggested using a Kerr cell together with a polarization controller. In the active Q-switching, the implementation of variable attenuators, such as mechanical device (chopper wheel), modulator (acousto-optic), electro-optic device (Pockels and Kerr cell) have achieved short pulse laser. In the passive Q-switching, an ion-doped crystal like Cr: YAG used for Nd: YAG (Klimov, Shcherbakov, & Tsvetkov, 1998) generates short pulse laser by the semiconductor. N₂-laser-pumped R6G dye laser has obtained the passive Q-switched pulse laser (Braverman, 1975) and 10.6 microns q-switching is generated by using a Co₂ laser (Bridges, 1966), A 678 ns pulse width is produced by using the Yb:GAB

crystal as the gain medium with Sb_2Te_3 saturable absorber at 1045.2 nm wavelength (X. Wang et al., 2017).

2.8 Overview of Mode-Locking Technique

Mode locking is an essential approach to the operation of laser light. It provides an ultrashort train of pulse laser in the range of femtoseconds. The basic working principle of mode-lock is locking all the phases that have slight differences in their frequencies. In other words, it locks the phases of all oscillating axial laser modes which leads to the emission of laser light as a train of ultrashort pulses, as illustrated in figure 2.12. The pulses duration, in the mode-locked, ranges from approximately 30 fs to 1 ns and in the range of 1 MHz to 100 GHz repetition rates. Indeed, mode-locked is one of the promising technologies that can generate an ultra-short pulse that is established with a semiconductor and solid-state lasers.

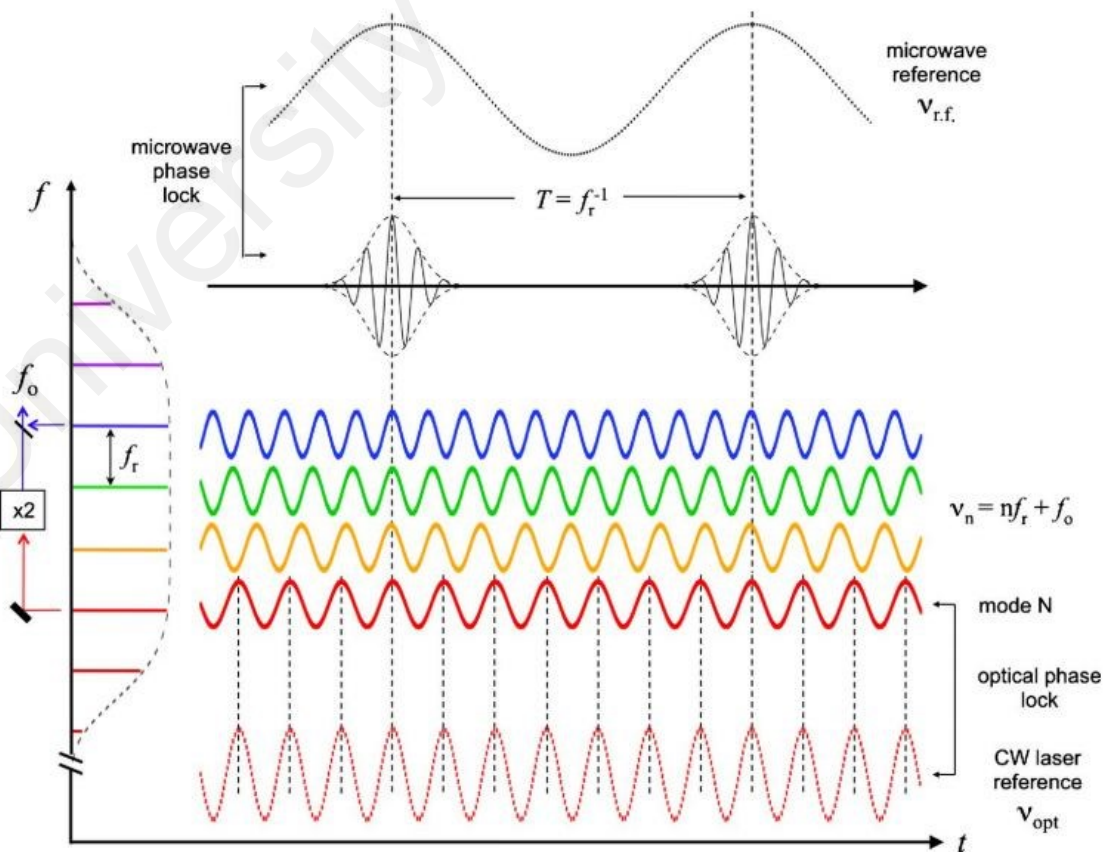


Figure 2.12: Mode-lock Operations

The novelty of mode-locked fiber laser is attributed to its compacted size, low cost and its simplicity which makes it applicable to various applications such as laser radar, THz generation, injection-seeding, optical telecommunications and others. Like the Q-switched, Mode-locked can be achieved by either active or passive technique.

The first technique applies some optical modulations that can manipulate the losses, an example of this modulation is the acousto-optic and electro-optic effects. The first achievement of the active mode-locked pulse laser was in 1964 by (Hargrove, Fork, & Pollack, 1964) that used the He–Ne laser. In 1972, a report was released which discarded the first generation of passive mode-locked that produced a pulse in Picosecond by using CW dye laser (Ippen, Shank, & Dienes, 1972). In 1992, the first significant result of passive mode locking, by using SESAMs, was achieved (Keller et al., 1996).

Recently, the growth of topological insulators (TI) was found to enhance the performance of the mode-lock pulse. In 2014, an investigation was performed on one of the IT family, specifically the Sb_2Te_3 saturable absorber, which generates a 1.8 ps pulse duration of the mode-lock by using the mechanically exfoliated technique (Jaroslaw Sotor et al., 2014b). In chapter 4, we experimentally demonstrated the performance of the mode-lock that uses the Sb_2Te_3 saturable absorber as a thin film for the first time to achieve 1 kW peak powers.

2.9 Liquid Phase Exfoliation (LPE) Technique

Liquid phase exfoliation (LPE) is another type used for the preparation of the 2D nanomaterials that breaks layered materials into 2D nanomaterials. A chosen solvent is added to the layered materials that is easy to suspend and break the material's crystal within the solvent. The LPE process depends on three general steps. These include: the

dispersion of the bulk material into the chosen solvent, the sonication and then the centrifugation. The propagation of high amplitude sonication waves in the sonication process induces shear forces and cavitation within the solution leading to the shearing of the crystal. Recently, this method has been widely used for the exfoliation of the layered materials such as black phosphorous and transition metal dichalcogenides (Gupta et al., 2016; Lin et al., 2017). Cui et al. have successfully fabricated the graphene using solvothermal-assisted exfoliation process in the acetonitrile (ACN) solvent, with the production of the graphene nanosheets (GNS) (Cui, Zhang, Hao, & Hou, 2011). The details of the mechanism of the solvothermal exfoliation processes of graphene is schematically illustrated in figure 2.13.

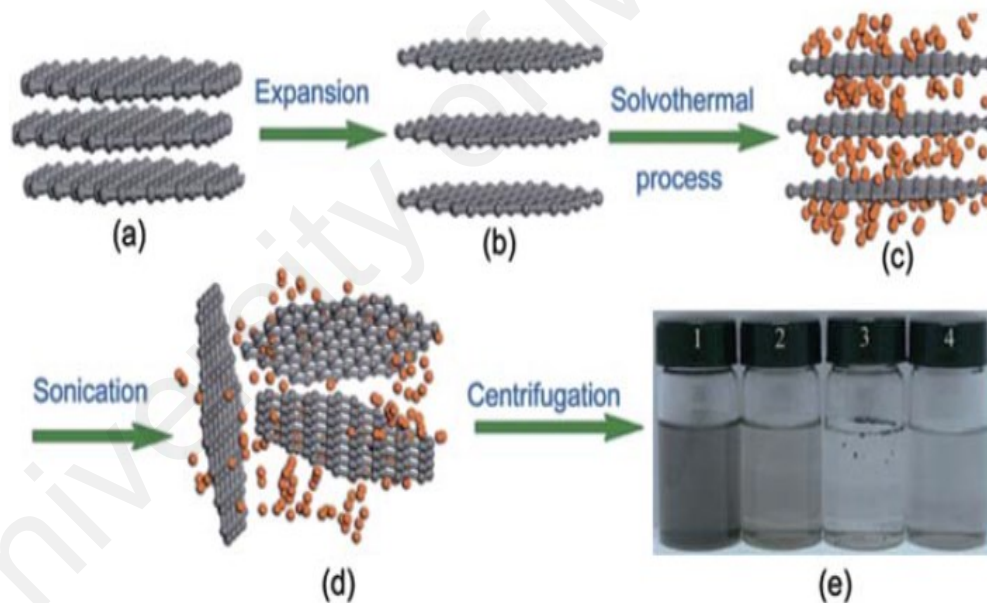


Figure 2.13: The solvothermal exfoliation processes

2.10 Optical Measurement

During the processes of pulse generation, various equipment and tools were used to measure and evaluate the laser performances. The Optical Spectrum Analyzer (OSA) (YOKOGAWA AQ6370C) was used to measure and display the distribution of power of

an optical source over a specified wavelength. The Digital Storage Oscilloscopes (GWInstek GDS-3352) was applied to graph an electrical signal as it varied over time, it was also used to record the repetition rate and the pulse width. The spectrum analyzer (Anritsu MS2683A) which was used in the experiment analyzed the wavelength spectrum and measured the SNR ratio. An Optical autocorrelation was implemented not only to measure the ultra-short pulse-width, especially for a pulse generated by mode-locking, but also to calculate the full width at half maximum. An Optical Power Meter (OMM-6810B) simultaneously measured the optical input and output power and wavelength of the laser cavity. A Laser Diode Pump was used as the input source for the laser cavity. The optical parameters were defined and calculated as shown below.

2.10.1 Repetition Rate and Pulse Duration

The pulse repetition frequency PRR is defined as the number of pulses or frequency of pulses of a repeating signal in a particular time unit, generally it is measured per second. In other words, when the pulse-duration (Δt) is very small (Pico, Femtosecond), the repetition rate R_r will be high. This has a broad range of applications (Ter-Mikirtychev, 2014). T is a pulse period, which can be calculated as

$$T = \frac{1}{\text{Repetition rate}, R_r} \quad (2.1)$$

Usually, mode-locked pulse laser produces ultrashort (femtosecond) pulse laser that has R_r in MHz and a few gigahertz. In Q-switching, the pulse-width is wider, this results in a Repetition rate in KHz. figure 2.14 presents the correlation between the R_r and pulse-duration.

2.10.2 Pulse Energy

Pulse energy E_p is the total amount of energy that is present in the optical pulse. When the average output power P_{out} increases, the pulse energy increases, in other words, the pulse energy is directly proportional to the average output power. However, repetition rate R_r is inversely proportional to the pulse energy. Pulse energy is calculated by

$$\text{Pulse energy } E_p \approx \frac{\text{average output power } (P_{out})}{\text{repetition rate } (R_r)} \quad (2.2)$$

2.10.3 Peak Power

Peak power P_p is the maximum level of the optical power which increases when the pulse-width decreases. In both of the Q-switching and mode-locking, the generated pulse-width is the range of Nano to Picosecond which produces a significant peak power. It can be calculated by

$$\text{Peak Power } P_p = \left(\frac{\text{energy } (E)}{\text{pulsewidth } (\Delta t)} \right) \quad (2.3)$$

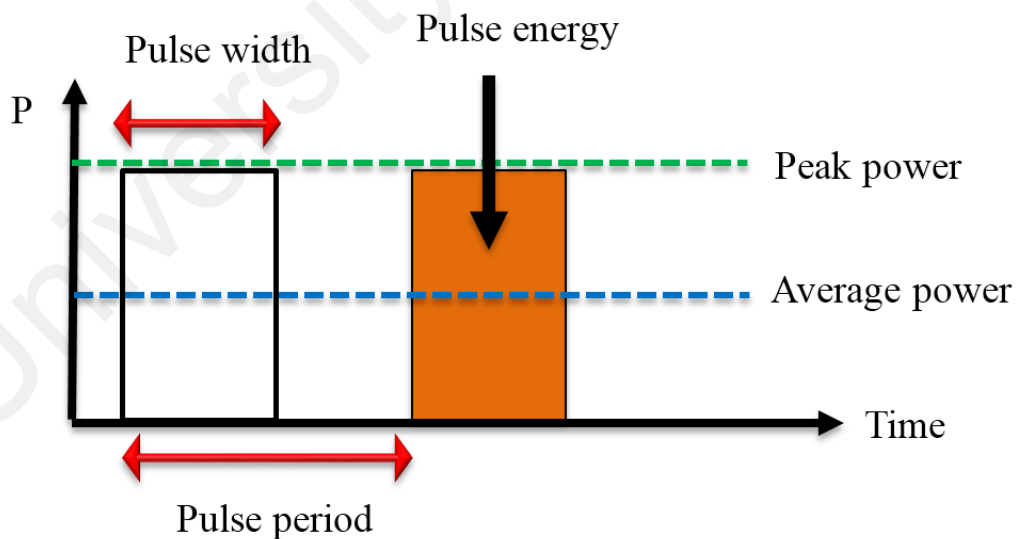


Figure 2.14: Repetition rate and pulse duration

CHAPTER 3: GENERATING Q-SWITCHED ERBIUM-DOPED FIBER LASERS USING ANTIMONY TELLURIDE SA

3.1 Introduction

The Q-switched erbium-doped fiber lasers (EDFLs) have attracted large research interests in the last few years specifically for its application in the field of optical communications. Furthermore, the Q-switched lasers have achieved a pulses train with high energy, narrow pulse width and high repetition rate and they can also be applicable for other applications such as medical diagnostics, fiber sensor and others. Under the passive technique of fiber laser, Q-switched gains more advantages over the active technique. The passive technique carries compensations of the low cost, the simplicity of laser cavity design and its operations (Ter-Mikirtychev, 2014). The Q-switched pulse laser is operated in the region of 1550 nm which is suitable for most of the optical communication. In this chapter, a Q-switched EDFL is demonstrated using an Antimony Telluride (Sb_2Te_3) as a saturable absorber.

3.2 Characterization and Fabrication of Antimony Telluride Sb_2Te_3

The saturable absorber was prepared by dissolving 5mg of the Sb_2Te_3 powder [Sigma Aldrich, -325 Mesh, 99.6% trace metal basis] into a solution of Polyvinyl alcohol (PVA) suspension with 120ml deionized water using the aid of a magnetic stirrer at room temperature. The mixture was stirred for 3 hours and was followed by ultra-sonication for an hour to prevent any aggregation. Then, the mixture was carefully poured into the petri dish and dried at room temperature for 3 days. The Sb_2Te_3 film had a thickness of 34 μm , as shown in figure 3.1. This process had various advantages such as clean growth

environment, crystal safety, low-growth temperature, organized thickness and being easy to dope (W. Tian, Yu, Shi, & Wang, 2017).

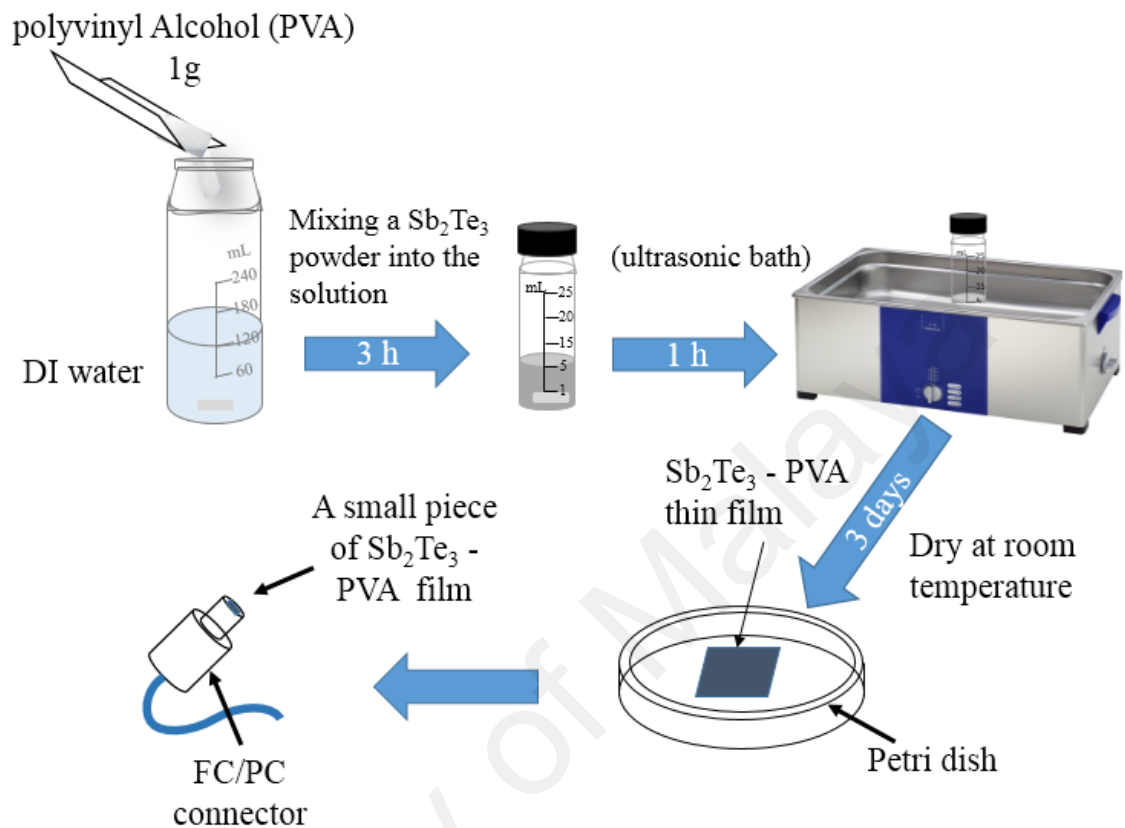


Figure 3.1: Fabrication processes of Antimony Telluride Sb₂Te₃

Figure 3.2 illustrates the FESEM image of the Sb₂Te₃ thin film, which shows diverse bumps on the surface. These formed bumps may result after drying the thin film at room temperature. The size of spherical-like shape was in the range between 0.2 to 1.33 μm . Figure 3.3 shows the linear absorbance spectrum of the Sb₂Te₃-PVA in the range between 200 to 1000 nm, which was obtained by using a broadband amplified spontaneous emission (ASE) light source and an optical spectrum analyzer. As shown in the figure, the linear absorption was characterized at the level of about 78 % by a flat profile. Figure 3.4 presents the Raman spectrum of the Sb₂Te₃-PVA film. It was obtained by using a diffraction grating of 1200 lines/mm with an excitation wavelength of 514 nm and laser

power of 10 mW. Two modes were shown at 2947.48 and 1433.18 cm^{-1} which were attributed to valence C-H vibration and shear modes for PVA polymer, respectively (C. Wang, Li, Ding, Xie, & Jiang, 2013).



Figure 3.2: Optical characteristics of the Sb_2Te_3 -PVA (FESEM image)

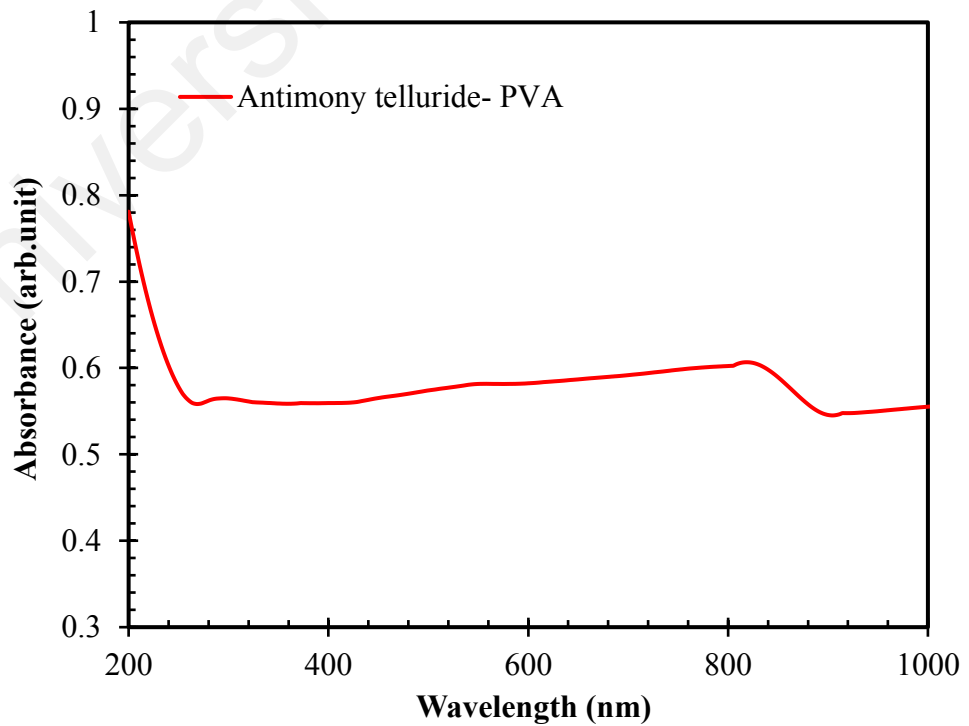


Figure 3.3: Linear absorption spectrum

An inset figure features four modes of Sb_2Te_3 at 49.52, 63.17, 106.72 and 171.68 cm^{-1} , corresponding to E_g^1 (TO), A_{1g}^1 (LO), E_g^2 (TO) and A_{1g}^2 (LO), respectively (J Sotor et al., 2014) and a peak at 133.84 cm^{-1} , which belongs to Te-Te bonds (packet structure) (Boguslawski et al., 2016). The nonlinear optical response property for the Sb_2Te_3 -PVA thickness were investigated to confirm its saturable absorption by applying a balanced twin-detector measurement technique. A self-constructed mode-locked fiber laser (1550 nm wavelength, 900 fs pulse-width, 17 MHz repetition rate) was used as the input pulse source. In this study, the transmitted power was recorded as a function of incident intensity on the device by varying the input laser power. The experimental data for transmission were fitted according to a simple two-level SA model of

$$T(I) = 1 - \alpha_s * \exp\left(\left(-\frac{I}{I_{sat}}\right) - \alpha_{ns}\right) \quad (3.1)$$

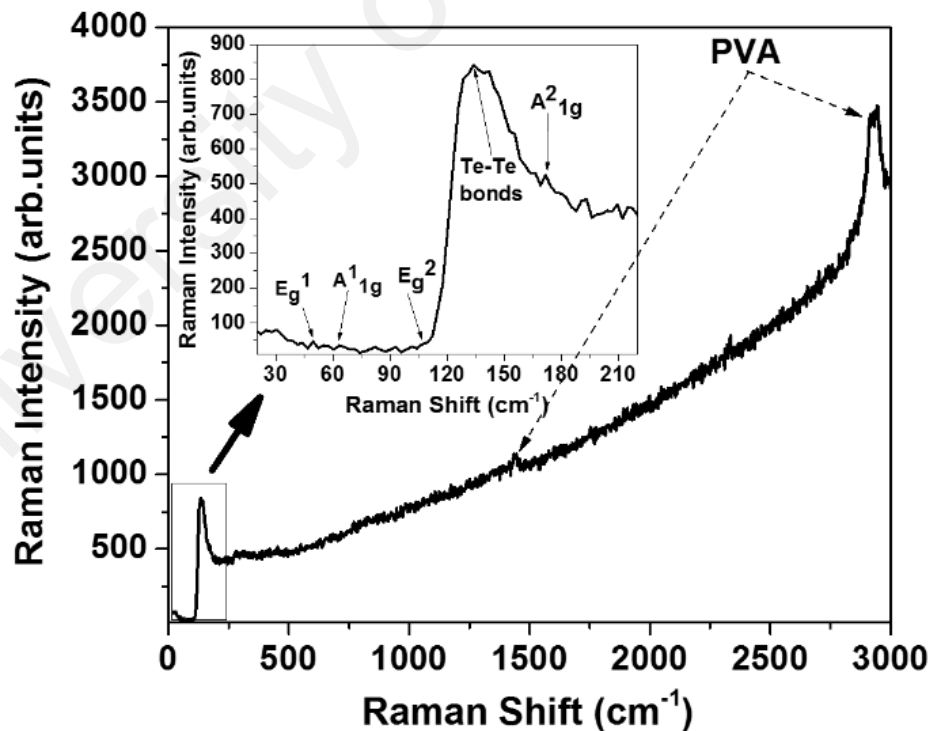


Figure 3.4: Raman spectrum

Where $T(I)$ is the transmission, α_s is the modulation depth, I is the input intensity, I_{sat} is the saturation intensity and α_{ns} is the non-saturable absorption. As shown in figure.

3.5, the modulation depth, non-saturable intensity and saturation intensity are obtained to be 8.5 %, 70 % and 36 MW/cm², respectively.

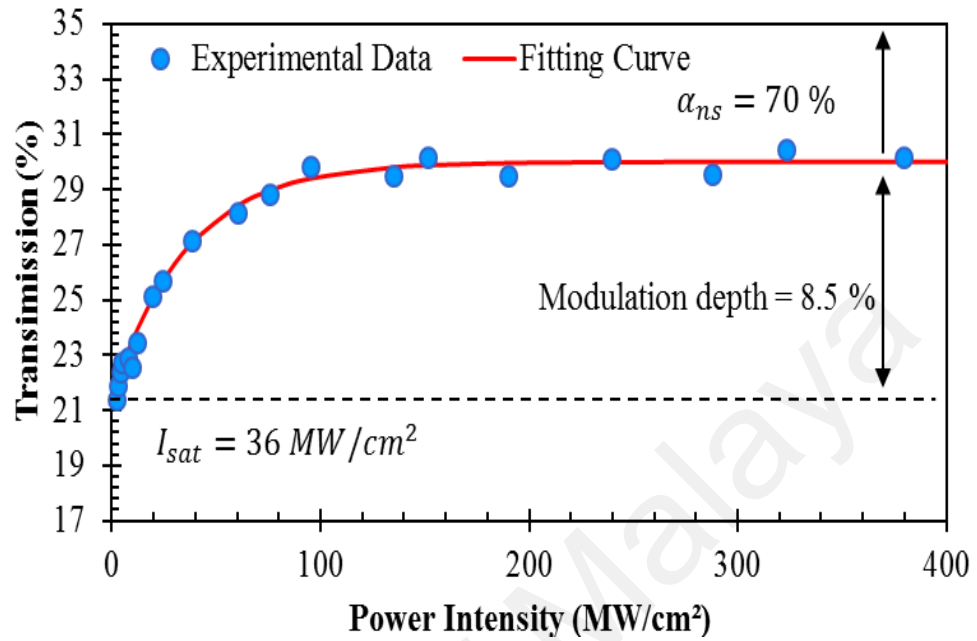


Figure 3.5: Nonlinear transmission

3.3 Laser Cavity Setup

The Antimony Telluride (Sb₂Te₃) – PVA composite was utilized to test and generate an ultrashort pulse laser. A Q-switching pulse laser EDFL was produced by a set of optical fiber equipment consisting of (980 nm Pump power, wavelength-division multiplexing (WDM), 3m EDF, Isolator, Coupler 80:20) as illustrated in figure 3.6. The Sb₂Te₃- PVA SA was placed into the fiber cavity by sandwiching ~ 1 mm² size piece of the film that was fabricated in the early stage and was placed between the two fiber connectors as demonstrated in the figure. 3.7. For a proper joint between the SA and the fiber connectors, the matching gel was applied. The total of the cavity length was 6 m which included EDF and 3 m of single mode fiber (SMF). The core diameter of EDF was 4 μm with 125 μm cladding diameter which had a numerical aperture of 0.16, Erbium ion absorption of 23 dB/m at 980 nm and group velocity dispersion (GVD) of 27.6 ps² km⁻¹. A 980nm laser diode was put into operation to the cavity as a pump source that went

through the wavelength-division multiplexing of 980/1550 nm. In order to avert any regressive laser reflection and to guarantee the unidirectional could propagate, an isolator was utilized in the cavity setup. A 80/20 coupler was placed to allow the 80% of the light propagate within the cavity and extract 20% of the signal outside the ring cavity which was attached to the diagnostics devices. The 20% output of the laser was connected to the 3dB coupler which was linked to the (OSA) optical spectrum analyzer and the (OSC) oscilloscope via the photodetector. For an additional important measurement the Radio Frequency (RF), the Optical Power Meter and the Autocorrelator were employed.

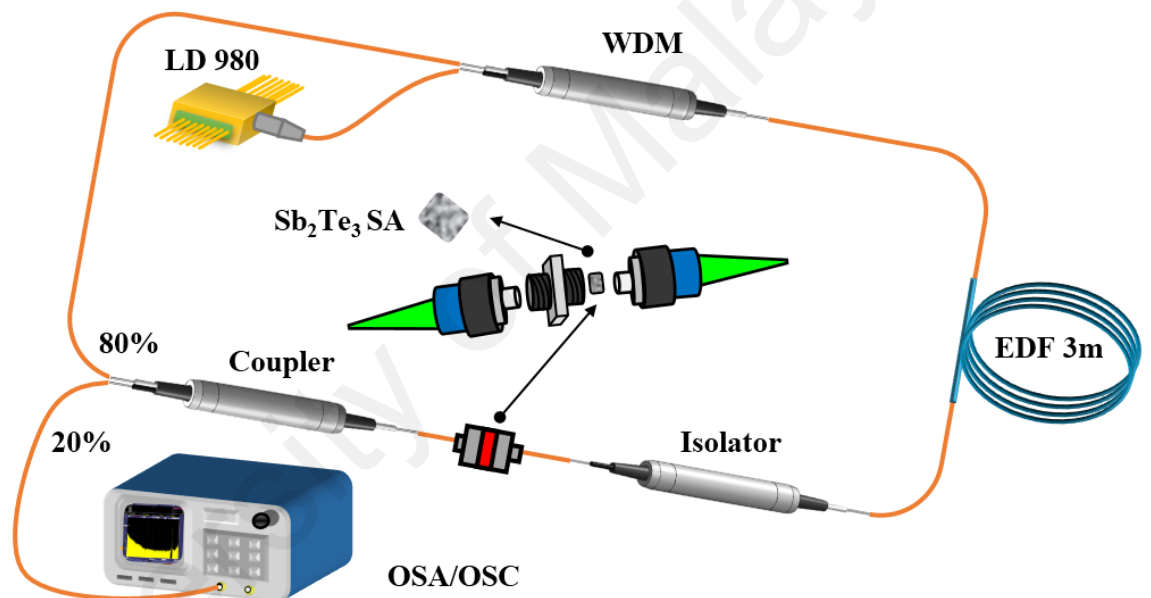


Figure 3.6: The ring cavity schematic diagram of the Q-Switched pulse laser with 4.9m total length

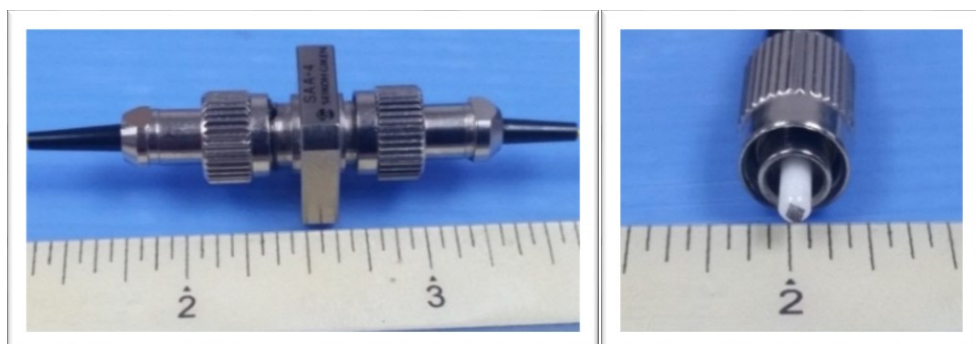


Figure 3.7: The fiber connectors of experiment with Sb₂Te₃ SA

3.4 Q-switched pulse laser performance

When the pump power reached low values of 10 mW, the continuous-wave laser was initiated. Consequently, the operation of the Q-switching pulses laser was initiated with a 15mW pump power threshold. With increasing the pump power, both of the pulse width and the repetition rate were changed accordingly which is the main property of the Q-switching pulse laser. Figure 3.8 indicates the Q-switch pulse laser that operated at 1530.749 nm Wavelength.

During the varies stages of the pump power, the laser pulse of Q-switched sustained with a stability between 15 mW to up to 81 mW. 27.53 kHz up to 95.06 kHz was the range of the repetition rate. Figure 3.9 demonstrates three different states of pump power with a repetition rate which were (15 mW - 27 kHz), (41 mW - 67 kHz) and (81 mW - 95 kHz) sequentially. This shows that the reputation rate increased and the pulse duration decreased proportionally with the increase of pump power. Figure 3.10 presents the power stability with 5.83% slope efficiency of pulse energy and the value output power associated with varies pump power stages. Figure 3.11 shows the relation between pulse width and repetition rate concurrently with different levels of the pump power.

When the pump power increased with its range, the pulse duration decreased from to 13.84 μ s to a minimum duration of 4.89 μ s. Figure 3.12 explains the relation between peak power and pulse duration corresponding to the pump power. Figure 3.13 features the measurement by the RF spectrum of 66.7 dB SNR Signal-to-noise ratio which was recorded at the maximum pump power. The cavity achieved a significant result with a low threshold pump power of 81 mW with a Pulse energy, Peak Power and Output Power of 45.86 nJ, 9.37mW and 4.36 Mw, respectively.

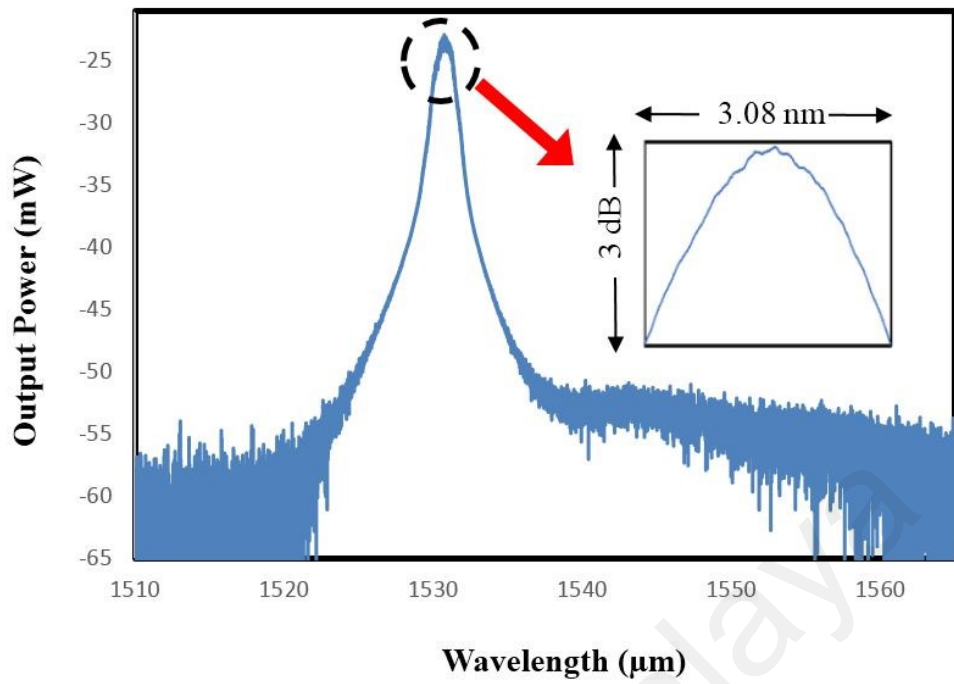


Figure 3.8 Stability of the Q-switching operations at 1533 nm wavelength

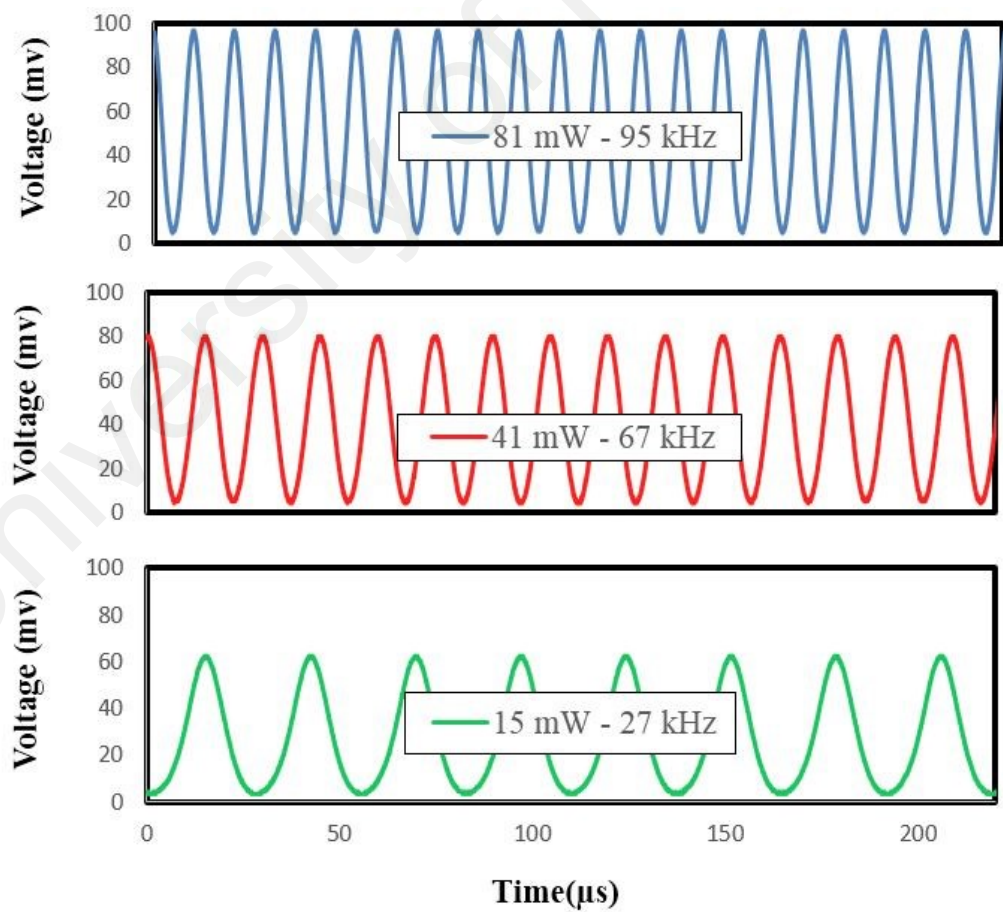


Figure 3.9: Oscilloscope train at pump power of 15 mW, 41 mW and 81 mW

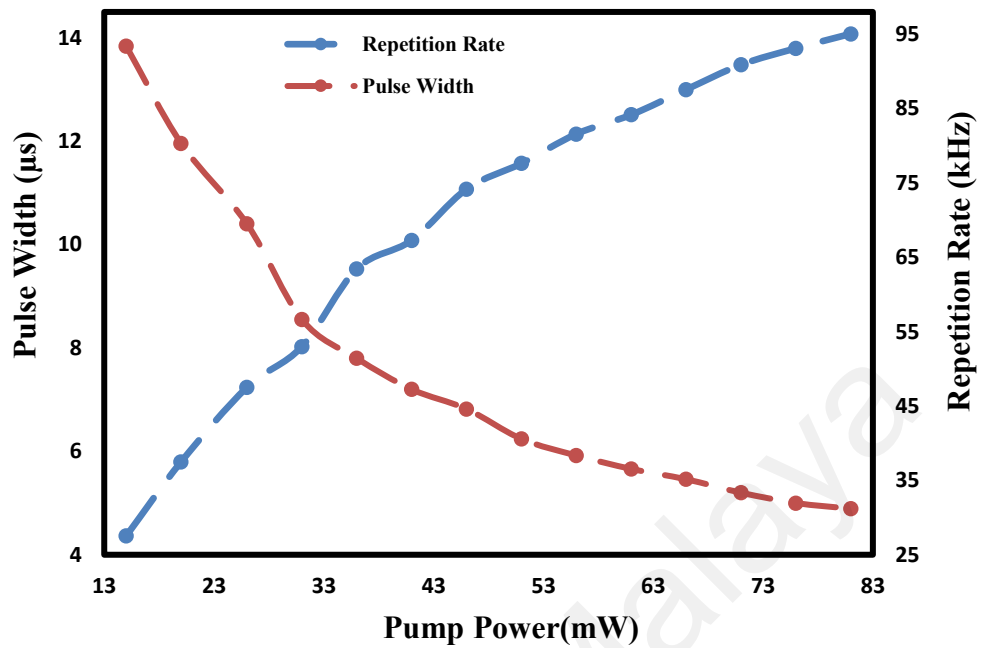


Figure 3.10: Pulse width and repetition rate at a various levels of the pump power.

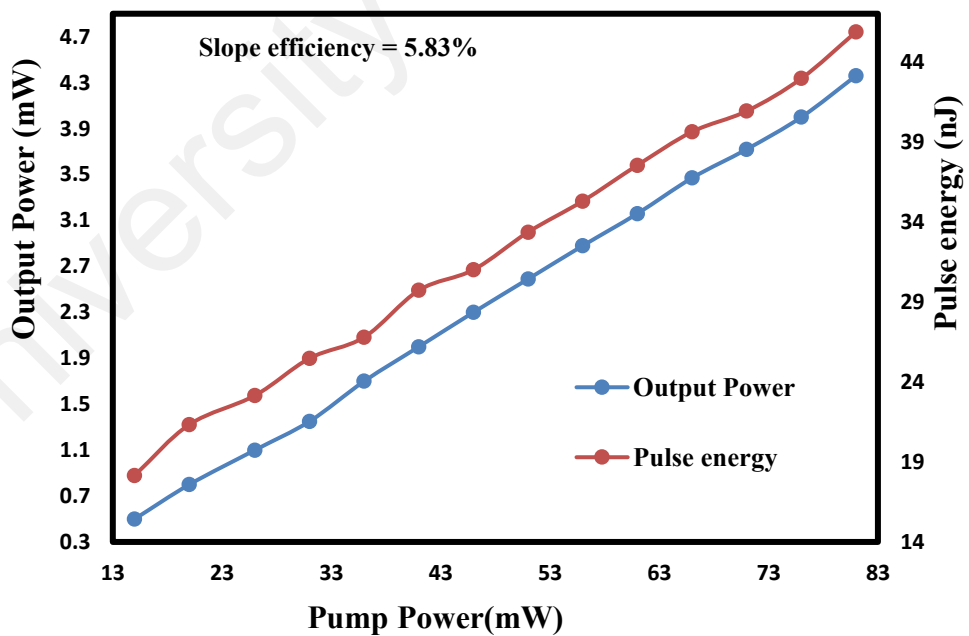


Figure 3.11: Pump power stability with 5.83% slope efficiency of pulse energy and output power.

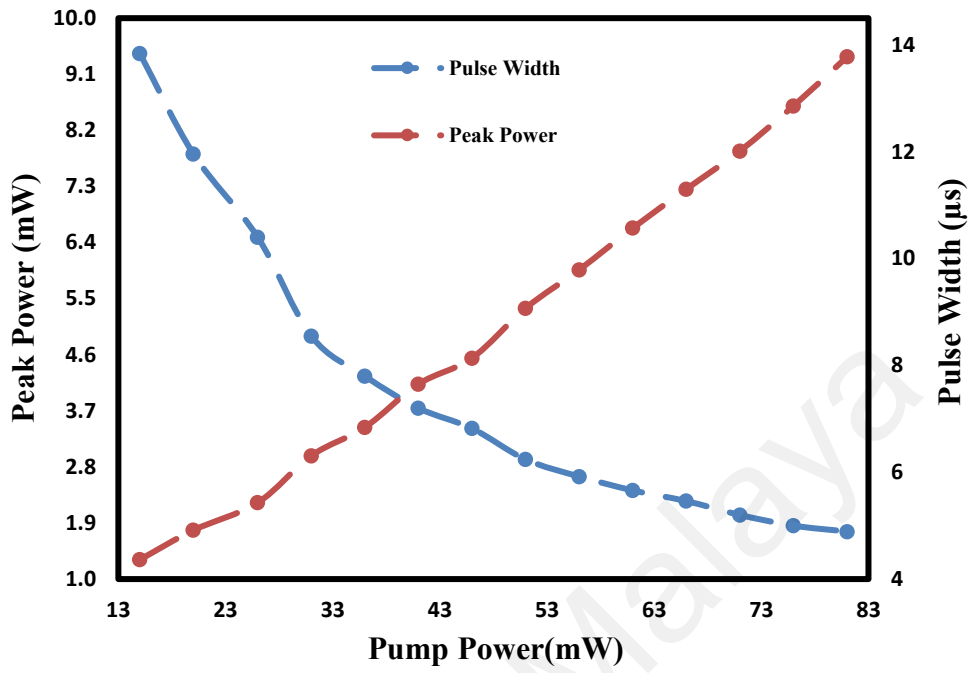


Figure 3.12: Peak power and pulse duration corresponding to the pump power

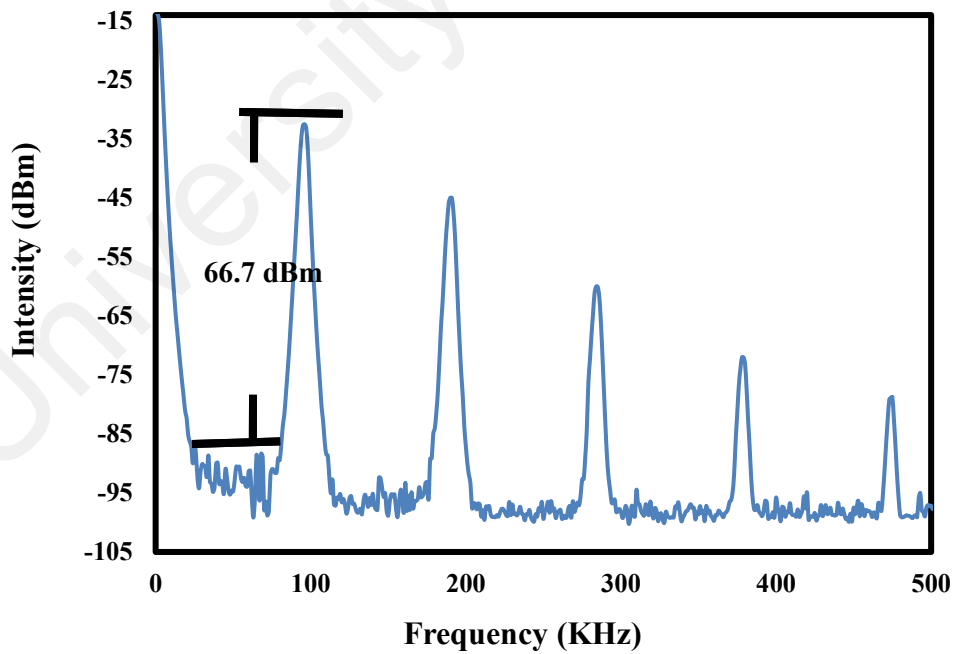


Figure 3.13: RF spectrum measurement

3.5 Summary

This chapter explained the fundamentals of Q-switched EDFLs, followed by the fabrication and characterization of Antimony Telluride (Sb_2Te_3) SA, that was embedded into polyvinyl alcohol (PVA) as a host polymer. The optical cavity setup and Q-switched operation were demonstrated. The Q-switched pulse laser was operated in the region of 1530.749 nm with a wavelength corresponding to 3.08 nm full-width at half maximum which was suitable for most of the optical communication. This SA was sandwiched between two fiber connectors inside the ring cavity. The operation of Q-switching pulses laser was initiated with a 15mW pump power threshold. Pump power and its repetition rate were demonstrated at three different states (15 mW - 27 kHz), (41 mW - 67 kHz) and (81 mW - 95 kHz) sequentially. The cavity achieved a significant result with a low threshold pump power of 81 mW. The pulse energy, peak Power and output Power were 45.86 nJ, 9.37mW and 4.36 Mw, respectively, and an RF spectrum of 66.7 dB SNR Signal-to-noise ratio which was recorded at the maximum pump power.

CHAPTER 4: GENERATING MODE-LOCKING ERBIUM-DOPED FIBER LASERS USING ANTIMONY TELLURIDE SA

4.1 Introduction

During recent years, the Mode-locked Erbium-doped fiber lasers, have been continuously investigating and achieving outstanding results. The novel achievement of Mode-locked is due its simplicity and the low cost of the laser cavity. Moreover, The produced pulse duration of Mode-locked is either in Picosecond or Femtosecond which is used to generate a significant beam of optical (ultrashort pulse lasers) with a high reputation rate (more than one MHz) (Ter-Mikirtychev, 2014). In this chapter, a mode-locked EDFLs was demonstrated using a simple and cheap Sb_2Te_3 SA. Liquid-phase exfoliation (LPE) was the method were the Sb_2Te_3 is fabricated using polyvinyl alcohol (PVA) as a host polymer. The fabricated saturable absorber was sandwiched between two fiber connectors inside the laser cavity.

4.2 Mode-Locked EDFL Setup and its performance

The mode-locked pulse laser was produced by a set of optical fiber equipment consisting of (980 nm Pump power, wavelength-division multiplexing (WDM), 3m EDF, Isolator, Coupler 80:20). The Sb_2Te_3 - PVA SA was placed into the fiber cavity by sandwiching a $\sim 1 \text{ mm}^2$ size piece of the film that was fabricated in the early stage and was placed between two fiber connectors. The cavity length was 6 m which included EDF and 3 m of single mode fiber (SMF) as shown in Figure 4.1. The core diameter of EDF was $4 \mu\text{m}$ with $125 \mu\text{m}$ cladding diameter which has a numerical aperture of 0.16.

This cavity differed from the Q-switched cavity setup by having a longer single mode fiber (SMF). The longer SMF provided sufficient nonlinearity and compensated the anomalous dispersion in the laser cavity (Reddy et al., 2018). The repetition rate could be reduced by using a longer cavity. As a result, the energy of the random pulse that emerged from the background noise as light propagated in the cavity can be increased. Therefore, by adding a long SMF cable to the ring cavity, the mode-locking could be promoted (Ismail et al., 2012).

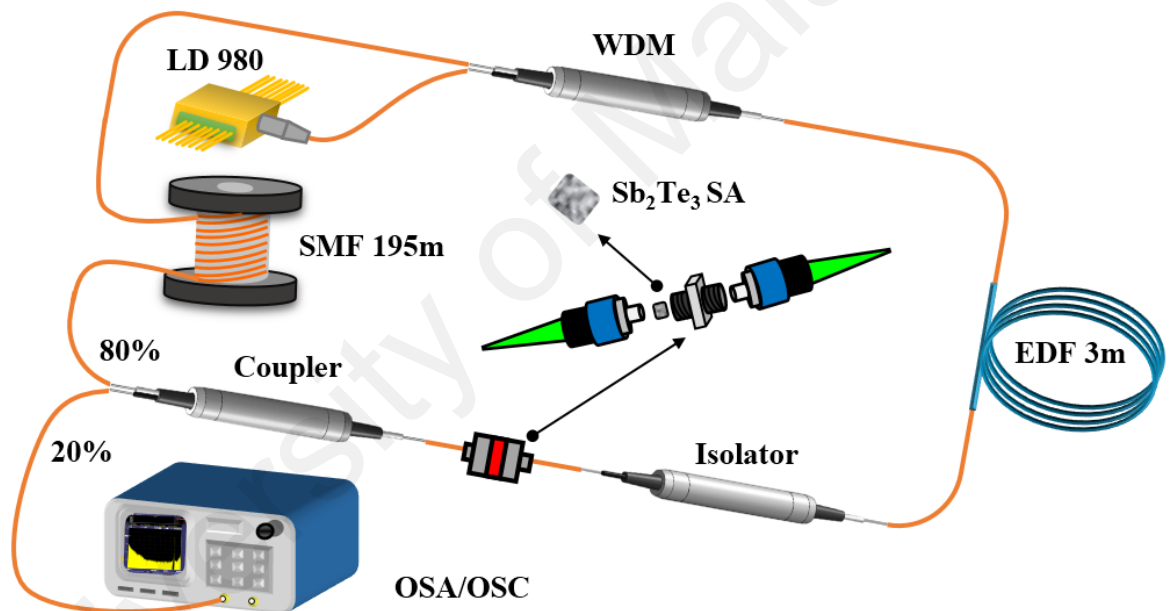


Figure 4.1: The ring cavity schematic diagram of the mode-locked pulsed laser with 201m total length

A mode-locking pulse laser was successfully generated by adding a single mode fiber (SMF) to the ring cavity which was 195 m length that had a group velocity dispersion

(GVD) of $-21.7 \text{ ps}^2 \text{ km}^{-1}$. The total of the cavity length was 201m with a total net dispersion of -4.2 ps^2 .

The self-starting mode-locked was initiated at 56 mW pump power as illustrated in Figure 4.3. The stabilized operation of the ultrashort pulses was obtained after 76 mW at 1533.40 nm wavelength with 2.7 nm FWHM as shown in Figure 4.2, which was measured by an optical spectrum analyzer (OSA). Figure 4.5 reveals a pulse energy that corresponding to the output power between the duration of 76 mW to a maximum threshold pump power of 143mW, which is obtained 4.51% slope efficiency. The repetition rate of the mode-locked was stabilized at a rate at 966 kHz from 76 mW pump power until it reaches its maximum values as shown in figure 4.3 and figure. 4.6. The minimum pulse width that was recorded was equal to 6.52 ps and was calculated by an Autocorrelator, which is presented in the figure. 4.4. The value of the major repetition rate was approved with the percentage of the signal-to-noise ratio of 67 dB, which was measured by RF spectrum analyzer as shown in the figure. 4.7. The accomplishment at a maximum threshold pump power of pulse energy, output power and peak power were 6.56 nJ, 6.50 mW and 1 kW respectively.

During the period of pulse generation there was no timing jitter or interrupt appeared in time-domain and frequency domain, also a stable single were observed. when it was applied inside the cavity. Therefore, the results were accomplished without using PC. No additional elements were required to generate both Q-switching and mode locking pulse laser.

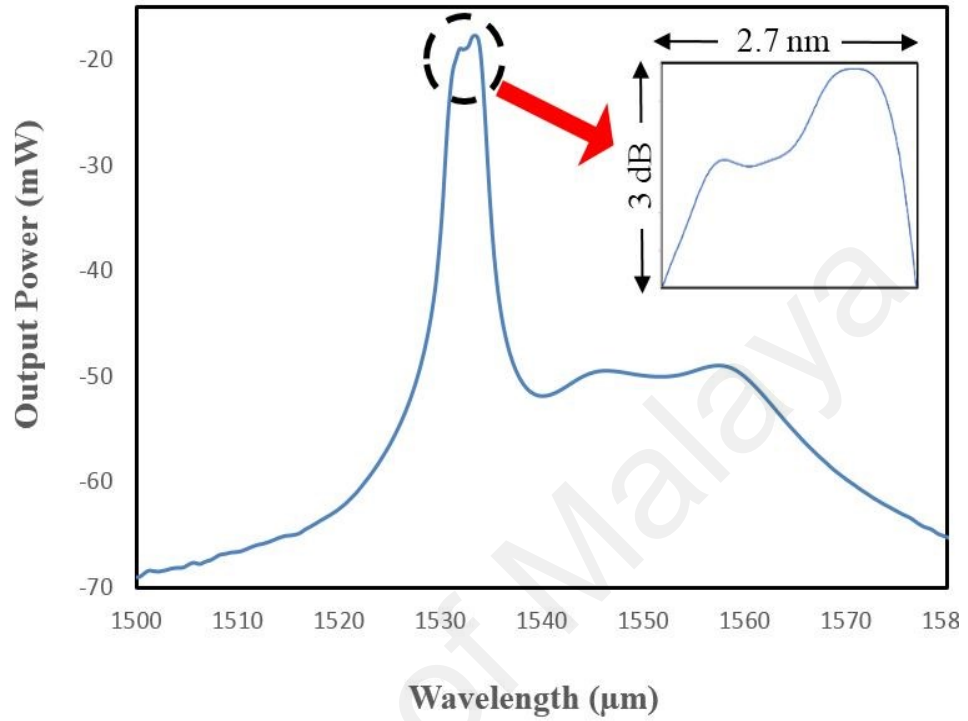


Figure 4.2: Mode-locked is operated at 1533.40 nm wavelength - 2.7 nm FWHM

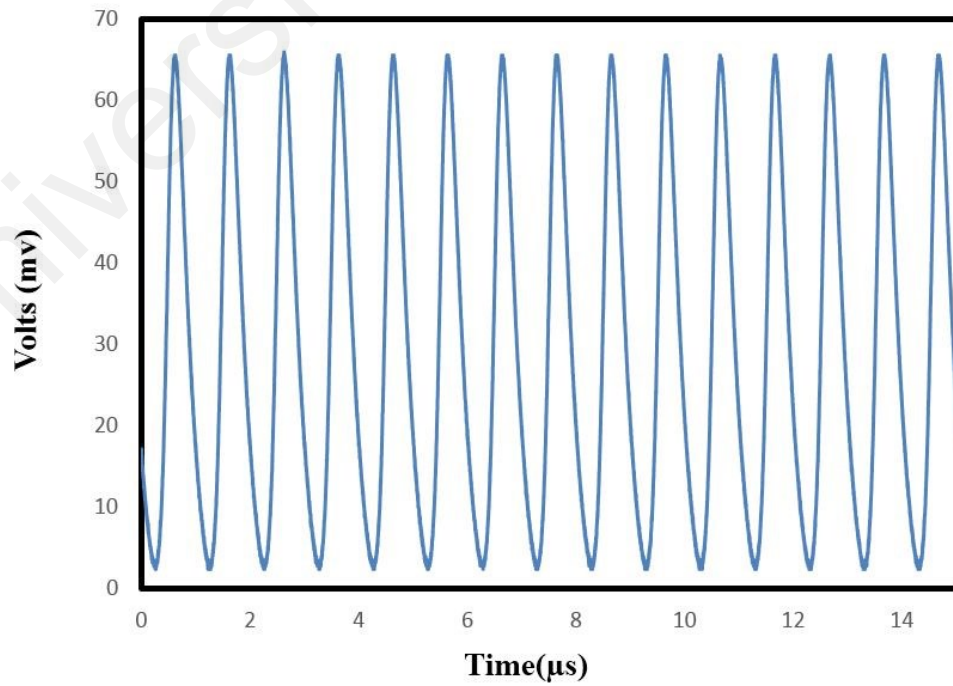


Figure 4.3: Oscilloscope output at maximum pump power

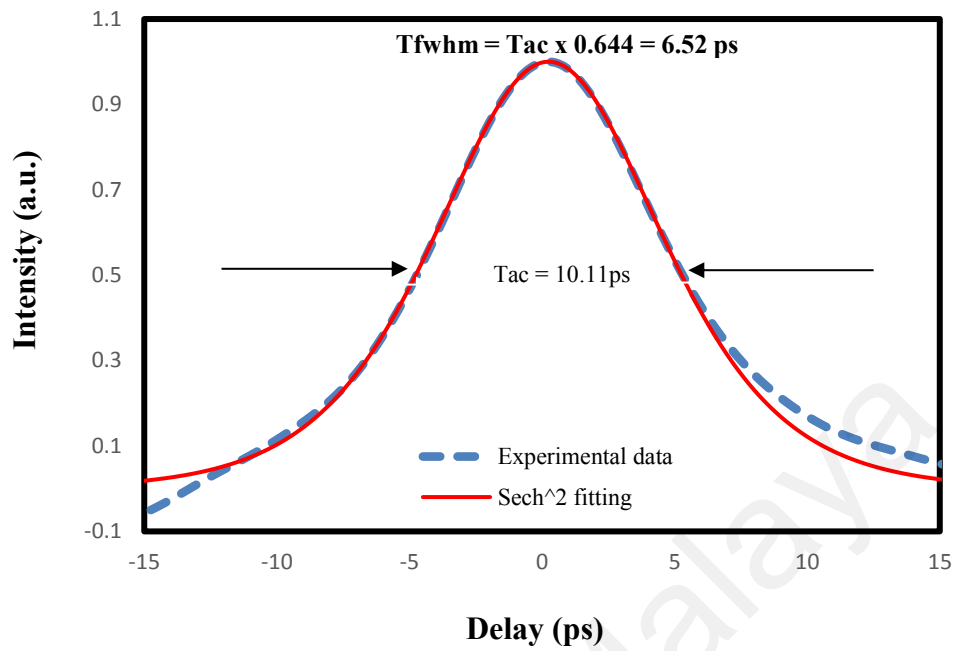


Figure 4.4: Autocorrelator pulse duration of 6.52 ps

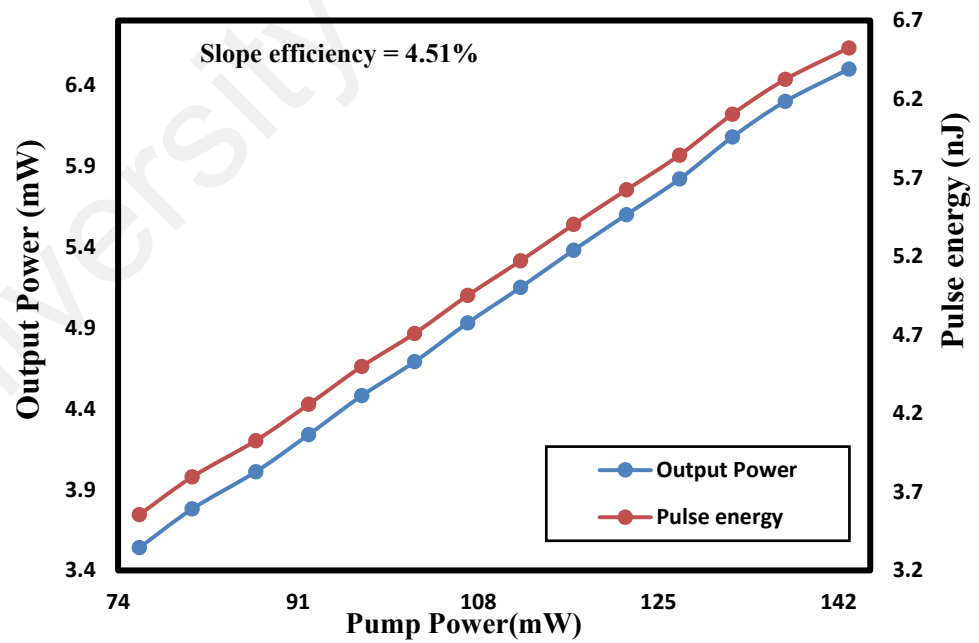


Figure 4.5: Pulse energy and output power with 4.51% slope efficiency during mode-locked operations

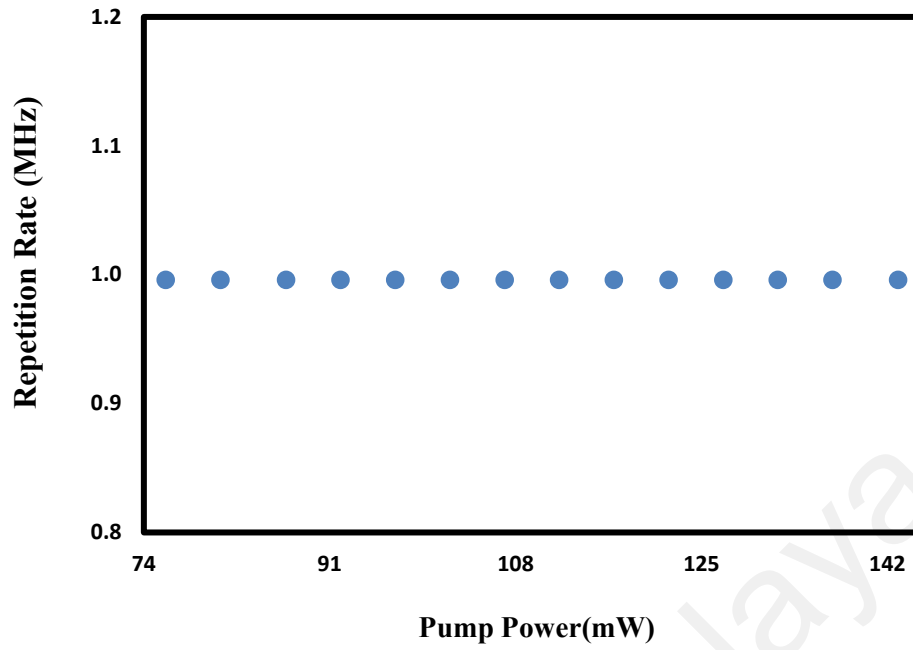


Figure 4.6: Repetition rate stability associated with pump power

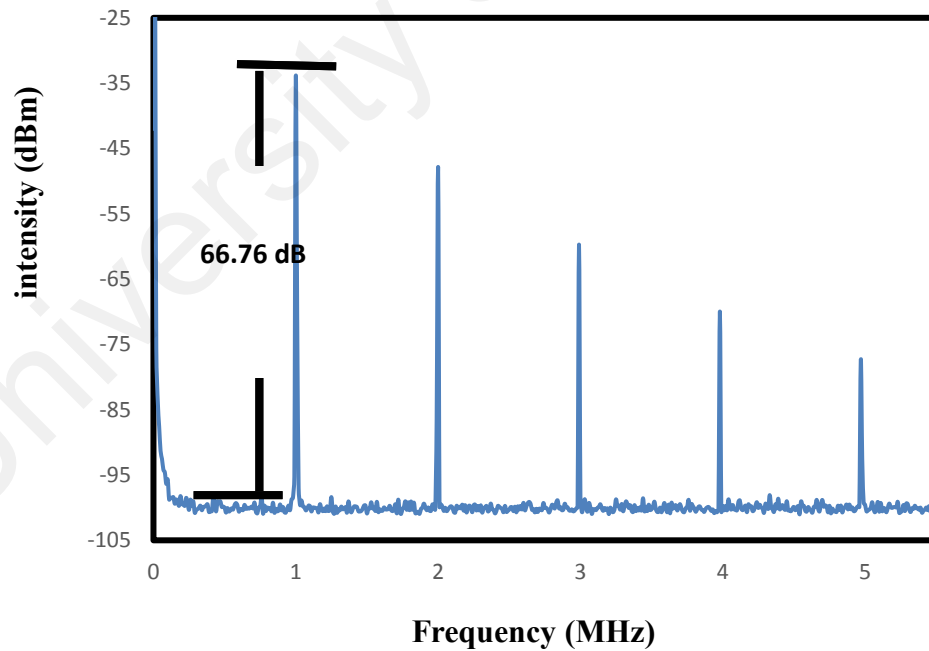


Figure 4.7: RF spectrum measurement with 66.76 dB SNR

4.3 Summary

This chapter described the accomplishment of mode-locked EDFLs by integrating the Antimony Telluride (Sb_2Te_3) SA, which was embedded into polyvinyl alcohol (PVA) as a host polymer. The Mode-locked laser cavity achieved a pulse width of 6.52 ps. Furthermore, it obtained a remarkable output power, pulse energy and peak power of 6.5 mW, 6.65 nJ and 1 kW respectively. The mode-locked pulse laser was operated in the region of 1533.40 nm with a 3dB bandwidth of 2.7 nm.

University of Malaya

CHAPTER 5: CONCLUSION

This report illustrated a compact, low-cost fiber pulse laser generated by both Q-switched and mode-locked EDFLs. The passive Q-switched and mode-locked EDFLs were experimentally demonstrated by implementing Antimony Telluride (Sb_2Te_3) Topological Insulator (TI) as a thin film saturable absorber (SA) which was embedded in polyvinyl alcohol (PVA) as a host polymer. Various applications were suitable for the achievement of the proposed laser performance.

The first objective was achieved by the fabrication of Antimony Telluride (Sb_2Te_3) SA of embedded in polyvinyl alcohol (PVA). Liquid phase exfoliation (LPE) method was used in the process of Sb_2Te_3 fabrication. The LPE technique of fabrication had a number of advantages such as crystal safety, clean growth environment, low-growth temperature, the its simplicity of the employment.

The proposed laser cavity in Q-switching had a total length of 6 m, a core diameter of EDF was 4 μm , 125 μm cladding diameter and 0.16a numerical aperture. Erbium ion absorption was 23 dB / m at 980 nm and the group velocity dispersion (GVD) of 27.6 $\text{ps}^2 \text{km}^{-1}$, while the cavity of mode-locking had a length of 201m with a total net dispersion of -4.2 ps^2 .

In a nutshell, the Q-switched pulse laser performance has a pulse laser at 81 mW threshold pump power. The accomplishment of Q-switched has a pulse energy, peak power, pulse width of 45.87 nJ, 9.37 mW and 4.89 μs , respectively. Chapter 4 demonstrated the mode-locking performance that had a pulse laser that was steadily produced from 71mW to 143mW pump power which induced a 6.52 ps pulse width with 996 KHz repetition rate. At a maximum pump power, the average output power was

approximately 6.5 mW, while the pulse energy and peak powers were 6.526 nJ and 1 kW, respectively.

The main achievement of this research was to generate a pulse laser with low pump threshold with a high pulse energy by using Antimony Telluride (Sb_2Te_3) as a thin film saturable absorber. Moreover, the pulse duration that was produced by mode-locking was in a picosecond. Outstandingly, the short pulse that was generated in the experiment, can contribute to the development of many fields such as medical diagnostics, bio-sensing, metrology and optical communication.

Although the achievement of this research seems promising, further in-depth studies should be carried out to improve the current research, especially in both gain medium of Ytterbium (Yb^{3+}) and Neodymium (Nd^{3+}) by using Antimony Telluride (Sb_2Te_3) SA. Moreover, other fabrication methods can be used to enhance the performance of pulse laser.

REFERENCES

- Agrawal, G. (2010). *Applications of nonlinear fiber optics*: Academic press.
- Ahmed, e. a. (2016). Femtosecond mode-locked erbium-doped fiber laser based on MoS₂-PVA saturable absorber. *Optics & Laser Technology*, 82, 145-149.
- Anwar, S., Anwar, S., & Mishra, B. K. (2014). Synthesis and Characterization of Bismuth Selenide Thin Films by Chemical Bath Deposition Technique. *Advanced Science Letters*, 20(3-4), 854-856.
- Aruldhas, G., & Rajagopal, P. (2005). *Modern physics*: PHI Learning Pvt. Ltd.
- Bertolotti, M. (2015). *Masers and lasers: a historical approach*: Crc Press.
- Bogusławski, J., Soboń, G., Tarnowski, K., Zybala, R., Mars, K., Mikula, A., . . . Sotor, J. (2016). All-polarization-maintaining-fiber laser Q-switched by evanescent field interaction with the Sb₂Te₃ saturable absorber. *Optical Engineering*, 55(8), 081316-081316.
- Braverman, L. (1975). Controlled passive Q switch for the N₂-laser-pumped dye laser. *Applied Physics Letters*, 27(11), 602-604.
- Bridges, T. (1966). COMPETITION, HYSTERESIS AND REACTIVE Q-SWITCHING IN CO₂ LASERS AT 10.6 MICRONS. *Applied Physics Letters*, 9(4), 174-176.
- Carruthers, T. F., Duling, I., & Dennis, M. L. (1994). Active-passive modelocking in a single-polarisation erbium fibre laser. *Electronics Letters*, 30(13), 1051-1053.
- Chang, Y. M., Lee, J., & Lee, J. H. (2012). Active mode-locking of an erbium-doped fiber laser using an ultrafast silicon-based variable optical attenuator. *Japanese Journal of Applied Physics*, 51(7R), 072701.
- Chen, X., Zhao, S., Zhao, J., Yang, K., Li, G., Li, D., . . . Feng, T. (2014). Sub-100ns passively Q-switched Nd: LuAG laser with multi-walled carbon nanotube. *Optics & Laser Technology*, 64, 7-10.
- Chen, Y.-C., Raravikar, N., Schadler, L., Ajayan, P., Zhao, Y.-P., Lu, T.-M., . . . Zhang, X.-C. (2002). Ultrafast optical switching properties of single-wall carbon nanotube polymer composites at 1.55 μm. *Applied Physics Letters*, 81(6), 975-977.
- Chen, Y., Jiang, G., Chen, S., Guo, Z., Yu, X., Zhao, C., . . . Tang, D. (2015). Mechanically exfoliated black phosphorus as a new saturable absorber for both Q-switching and mode-locking laser operation. *Optics express*, 23(10), 12823-12833.
- Chow, W. W., & Koch, S. W. (2013). *Semiconductor-laser fundamentals: physics of the gain materials*: Springer Science & Business Media.

- Cizmeciyan, M., Kim, J., Bae, S., Hong, B., Rotermund, F., & Sennaroglu, A. (2013). Graphene mode-locked femtosecond Cr: ZnSe laser at 2500 nm. *Optics letters*, 38(3), 341-343.
- Cui, X., Zhang, C., Hao, R., & Hou, Y. (2011). Liquid-phase exfoliation, functionalization and applications of graphene. *Nanoscale*, 3(5), 2118-2126.
- DeCusatis, C., & DeCusatis, C. J. S. (2010). *Fiber optic essentials*: Academic Press.
- Dong, L., & Samson, B. (2016). *Fiber Lasers: Basics, Technology, and Applications*: Crc Press.
- Dutta, N. K. (2015). *Fiber amplifiers and fiber lasers*: World Scientific.
- Gambling, W. A. (1992). Optical fibres, lasers, and amplifiers. *Endeavour*, 16(1), 17-22.
- Gupta, A., Arunachalam, V., & Vasudevan, S. (2016). Liquid-Phase Exfoliation of MoS₂ Nanosheets: The Critical Role of Trace Water. *The journal of physical chemistry letters*, 7(23), 4884-4890.
- Hargrove, L., Fork, R. L., & Pollack, M. (1964). Locking of He-Ne laser modes induced by synchronous intracavity modulation. *Applied Physics Letters*, 5(1), 4-5.
- Hasan, M. Z., & Moore, J. E. (2011). Three-dimensional topological insulators. *Annu. Rev. Condens. Matter Phys.*, 2(1), 55-78.
- Hellwarth, R. (1961). *Advances in quantum electronics*: Columbia Press, New York.
- Ippen, E., Shank, C., & Dienes, A. (1972). Passive mode locking of the cw dye laser. *Applied Physics Letters*, 21(8), 348-350.
- Ismail, M. A., Harun, S. W., Zulkepely, N. R., Nor, R. M., Ahmad, F., & Ahmad, H. (2012). Nanosecond soliton pulse generation by mode-locked erbium-doped fiber laser using single-walled carbon-nanotube-based saturable absorber. *Applied Optics*, 51(36), 8621-8624.
- Jung, M., Koo, J., Park, J., Song, Y.-W., Jhon, Y. M., Lee, K., . . . Lee, J. H. (2013). Mode-locked pulse generation from an all-fiberized, Tm-Ho-codoped fiber laser incorporating a graphene oxide-deposited side-polished fiber. *Optics express*, 21(17), 20062-20072.
- Keller, U. (2003). Recent developments in compact ultrafast lasers. *Nature*, 424(6950), 831-838.
- Keller, U., Weingarten, K. J., Kartner, F. X., Kopf, D., Braun, B., Jung, I. D., . . . Der Au, J. A. (1996). Semiconductor saturable absorber mirrors (SESAM's) for femtosecond to nanosecond pulse generation in solid-state lasers. *IEEE Journal of selected topics in QUANTUM ELECTRONICS*, 2(3), 435-453.
- Kim, H., Cho, J., Jang, S.-Y., & Song, Y.-W. (2011). Deformation-immunized optical deposition of graphene for ultrafast pulsed lasers. *Applied Physics Letters*, 98(2), 021104.

- Klimov, I., Shcherbakov, I., & Tsvetkov, V. (1998). Control of the Nd-laser output by Cr-doped Q-switches. *LASER PHYSICS-LAWRENCE-*, 8, 232-237.
- Kong, D., Dang, W., Cha, J. J., Li, H., Meister, S., Peng, H., . . . Cui, Y. (2010). Few-layer nanoplates of Bi₂Se₃ and Bi₂Te₃ with highly tunable chemical potential. *Nano letters*, 10(6), 2245-2250.
- Kowalczyk, M., Bogusławski, J., Zybala, R., Mars, K., Mikuła, A., Soboń, G., & Sotor, J. (2016). Sb₂Te₃-deposited D-shaped fiber as a saturable absorber for mode-locked Yb-doped fiber lasers. *Optical materials express*, 6(7), 2273-2282.
- Lin, S., Chui, Y., Li, Y., & Lau, S. P. (2017). Liquid-phase exfoliation of black phosphorus and its applications. *FlatChem*, 2, 15-37.
- Liu, X., Smith, D., Fan, J., Zhang, Y.-H., Cao, H., Chen, Y., . . . Furdyna, J. (2011). Structural properties of Bi₂Te₃ and Bi₂Se₃ topological insulators grown by molecular beam epitaxy on GaAs (001) substrates. *Applied Physics Letters*, 99(17), 171903.
- Luo, Z., Zhou, M., Weng, J., Huang, G., Xu, H., Ye, C., & Cai, Z. (2010). Graphene-based passively Q-switched dual-wavelength erbium-doped fiber laser. *Optics letters*, 35(21), 3709-3711.
- Maiman, T. H. (1960). Stimulated optical radiation in ruby. *Nature*, 187(4736), 493-494.
- Mao, Q., & Lit, J. W. (2003). Multiwavelength erbium-doped fiber lasers with active overlapping linear cavities. *Journal of lightwave technology*, 21(1), 160-169.
- Martinez, A., Fuse, K., & Yamashita, S. (2013). Enhanced stability of nitrogen-sealed carbon nanotube saturable absorbers under high-intensity irradiation. *Optics express*, 21(4), 4665-4670.
- McClung, F., & Hellwarth, R. (1962). Giant optical pulsations from ruby. *Applied Optics*, 1(101), 103-105.
- Pan, L., Utkin, I., & Fedosejevs, R. (2007). Passively Q-switched Ytterbium-Doped Double-Clad Fiber Laser With a Cr⁴⁺: YAG Saturable Absorber. *IEEE Photonics technology letters*, 19(24), 1979-1981.
- Patel, C. K. N. (1964). Continuous-Wave Laser Action on Vibrational-Rotational Transitions of CO₂. *Physical review*, 136(5A), A1187.
- Popa, D., Sun, Z., Hasan, T., Torrisi, F., Wang, F., & Ferrari, A. (2011). Graphene Q-switched, tunable fiber laser. *Applied Physics Letters*, 98(7), 073106.
- Popa, D., Sun, Z., Torrisi, F., Hasan, T., Wang, F., & Ferrari, A. (2010). Sub 200 fs pulse generation from a graphene mode-locked fiber laser. *Applied Physics Letters*, 97(20), 203106.
- Reddy, P. H., Rahman, M., Paul, M., Latiff, A., Rosol, A., Das, S., . . . Harun, S. (2018). Titanium Dioxide Doped Fiber as a New Saturable Absorber for Generating

Mode-Locked Erbium Doped Fiber Laser. *Optik-International Journal for Light and Electron Optics*.

- Savage, N. (2010). Acousto-optic devices. *Nature photonics*, 4(10), 728-729.
- Siegman, A. E. (2000). Laser beams and resonators: The 1960s. *IEEE Journal of selected topics in QUANTUM ELECTRONICS*, 6(6), 1380-1388.
- Sotor, J., Sobon, G., Grodecki, K., & Abramski, K. (2014). Mode-locked erbium-doped fiber laser based on evanescent field interaction with Sb_2Te_3 topological insulator. *Applied Physics Letters*, 104(25), 251112.
- Sotor, J., Sobon, G., Macherzynski, W., Paletko, P., & Abramski, K. M. (2015). Black phosphorus saturable absorber for ultrashort pulse generation. *Applied Physics Letters*, 107(5), 051108.
- Sotor, J., Sobon, G., Macherzynski, W., Paletko, P., Grodecki, K., & Abramski, K. M. (2014a). Mode-locking in Er-doped fiber laser based on mechanically exfoliated Sb_2Te_3 saturable absorber. *Optical materials express*, 4(1), 1-6.
- Sotor, J., Sobon, G., Macherzynski, W., Paletko, P., Grodecki, K., & Abramski, K. M. (2014b). Mode-locking in Er-doped fiber laser based on mechanically exfoliated Sb_2Te_3 saturable absorber. *Optical Materials Express*, 4(1), 1-6.
- Strickland, D., & Mourou, G. (1985). Compression of amplified chirped optical pulses. *Optics communications*, 55(6), 447-449.
- Ter-Mikirtychev, V. V. (2014). *Fundamentals of fiber lasers and fiber amplifiers*: Springer.
- Tian, L., Xu, Z., Zhao, S., Cui, Y., Liang, Z., Zhang, J., & Xu, X. (2014). The Upconversion Luminescence of $\text{Er}^{3+}/\text{Yb}^{3+}/\text{Nd}^{3+}$ Triply-Doped $\beta\text{-NaYF}_4$ Nanocrystals under 808-nm Excitation. *Materials*, 7(11), 7289-7303.
- Tian, W., Yu, W., Shi, J., & Wang, Y. (2017). The Property, Preparation and Application of Topological Insulators: A Review. *Materials*, 10(7), 814.
- Träger, F. (2012). *Springer handbook of lasers and optics*: Springer Science & Business Media.
- Wang, C., Li, Y., Ding, G., Xie, X., & Jiang, M. (2013). Preparation and characterization of graphene oxide/poly (vinyl alcohol) composite nanofibers via electrospinning. *Journal of Applied Polymer Science*, 127(4), 3026-3032.
- Wang, X., Xu, J., Sun, Y., Zhu, Z., You, Z., & Tu, C. (2017). Near infrared passively Q-switched solid state laser based on Sb_2Te_3 topological insulator saturable absorber. *Journal of Luminescence*.

LIST OF PUBLICATIONS AND PAPERS PRESENTED

- AL-DABAGH, Z. A. I., AHMED, M. H. M., AL-MASOODI, A. H. H., LATIFF, A. A., HARUN, S. W. (2017), Q-Switched and Mode-Locked Erbium-Doped Fiber Lasers Using Antimony Telluride (Sb_2Te_3) Saturable Absorber, *Applied Optics* (submitted).

University of Malaya